Version of record at: https://doi.org/10.1029/ 2024JG008478

JGR Biogeosciences

RESEARCH ARTICLE
10.1029/2024JG008478

Key Points:

- Methanogenesis and sulfate-reduction co-occur as a result of methylotrophic methanogenesis
- Methylotrophic methanogenesis was an important methanogenic pathway in high sulfide environments
- Methanotrophs had higher relative abundances in environments with lower sulfide levels

Supporting Information:

Supporting Information may be found in the online version of this article.

Correspondence to:

M. J. Wilkins,
mike.wilkins@colostate.edu

Citation:

Bechtold, E. K., Xin, D., Pacheco, M., Toner, B. M., Arnold, W. A., Chin, Y.-P., & Wilkins, M. J. (2025). Diverse cooccurring metabolisms support sulfur and methane cycling in wetland surficial sediments. *Journal of Geophysical Research: Biogeosciences*, *130*, e2024JG008478. https://doi.org/10.1029/2024JG008478

Received 17 SEP 2024
Accepted 25 AUG 2025

Author Contributions:

Conceptualization: Emily K. Bechtold, Danhui Xin, Michael J. Wilkins
Formal analysis: Emily K. Bechtold, Danhui Xin, Maricia Pacheco, Brandy M. Toner
Funding acquisition: Brandy M. Toner, William A. Arnold, Yu-Ping Chin, Michael J. Wilkins
Investigation: Emily K. Bechtold
Methodology: Emily K. Bechtold, Danhui Xin, Maricia Pacheco
Project administration: Michael J. Wilkins
Resources: William A. Arnold, Yu-Ping Chin, Michael J. Wilkins
Supervision: Brandy M. Toner, William A. Arnold, Yu-Ping Chin, Michael J. Wilkins

Diverse Cooccurring Metabolisms Support Sulfur and Methane Cycling in Wetland Surficial Sediments

Emily K. Bechtold[1], Danhui Xin[2,3], Maricia Pacheco[4,5], Brandy M. Toner[4], William A. Arnold[5], Yu-Ping Chin[2], and Michael J. Wilkins[1]

[1]Department of Soil and Crop Sciences, Colorado State University, Fort Collins, CO, USA, [2]Department of Civil and Environmental Engineering, University of Delaware, Newark, DE, USA, [3]Now at Southern California Coastal Water Research Project Authority, Costa Mesa, CA, USA, [4]Department of Soil, Water, and Climate, University of Minnesota-Twin Cities, Minneapolis, MN, USA, [5]Department of Civil, Environmental, and Geo- Engineering, University of Minnesota, Minneapolis, MN, USA

Abstract The Prairie Pothole Region (PPR) of North America contains millions of small depressional wetlands with some of the highest methane (CH_4) fluxes ever reported in terrestrial ecosystems. In saturated soils, two conventional paradigms are (a) methanogenesis is the final step in the redox ladder, occurring only after more thermodynamically favorable electron acceptors (e.g., sulfate) are reduced, and (b) CH_4 is primarily produced by acetoclastic and hydrogenotrophic pathways. However, previous work in PPR wetlands observed co-occurrence of sulfate-reduction and methanogenesis and the presence of diverse methanogenic substrates (i.e., methanol, DMS). This study investigated how methylotrophic methanogenesis—in addition to acetoclastic and hydrogenotrophic methanogenesis—significantly contributes to CH_4 flux in surface sediments and thus allows for the co-occurrence of competing redox processes in PPR sediments. We addressed this aim through field studies in two distinct high CH_4 emitting wetlands in the PPR complex, which coupled microbial community compositional and functional inferences with depth-resolved electrochemistry measurements in surficial wetland sediments. This study revealed methylotrophic methanogens as the dominant group of methanogens in the presence of abundant organic sulfate esters, which are likely used for sulfate reduction. Resulting high sulfide concentrations likely caused sulfide toxicity in hydrogenotrophic and acetoclastic methanogens. Additionally, the use of non-competitive substrates by many methylotrophic methanogens allows these metabolisms to bypass thermodynamic constraints and can explain co-existence patterns of sulfate-reduction and methanogenesis. This study demonstrates that the current models of methanogenesis in wetland ecosystems insufficiently represent carbon cycling in some of the highest CH_4 emitting environments.

Plain Language Summary Atmospheric methane (CH_4), a potent greenhouse gas (GHG) responsible for approximately 20% of current atmospheric warming, is rising at faster rates than other GHGs such as CO_2. Causes of this rise are not well understood but hypothesized to be in part due to increased emissions from wetlands, the largest natural source of global CH_4 emissions. The Prairie Pothole Region (PPR), the 10th largest global wetland complex, comprises millions of small depressional wetlands. These wetlands have some of the highest levels of sulfate reduction and methanogenesis recorded in terrestrial ecosystems, but the mechanisms driving such high levels of CH_4 production are poorly understood. This study revealed that methylotrophic methanogens—in contrast to more intensively studied acetoclastic and hydrogenotrophic methanogens—can be dominant in PPR sediments. Due to their metabolism, these methanogens can co-occur with other anaerobic bacteria such as sulfate reducers, and therefore likely contribute to high rates of methane generation. These findings contribute to our understanding of methanogenesis in natural wetlands and can inform climate models allowing us to better understand and predict future atmospheric warming.

1. Introduction

Wetland ecosystems represent the largest natural source of methane (CH_4), a potent greenhouse gas (GHG), accounting for 20%–50% of global CH_4 emissions (Bridgham et al., 2013; Laanbroek, 2010; Rosentreter et al., 2021). Wetland size is an important factor in CH_4 flux, with rates increasing as wetland size decreases; indeed, small ponds (surface area <0.001 km^2) are estimated to contribute up to 40% of CH_4 emissions from inland freshwater ecosystems (Bansal et al., 2023; Holgerson & Raymond, 2016). The Prairie Pothole Region (PPR), located in the Great Plains of North America, is one of the world's largest inland wetland ecosystems

Journal of Geophysical Research: Biogeosciences 10.1029/2024JG008478

Visualization: Emily K. Bechtold, Danhui Xin
Writing – original draft: Emily K. Bechtold, Danhui Xin, Brandy M. Toner
Writing – review & editing: Emily K. Bechtold, Maricia Pacheco, Brandy M. Toner, William A. Arnold, Yu-Ping Chin, Michael J. Wilkins

spanning ∼820,000 km^2 and is comprised of millions of depressional wetlands that are hydrologically connected by groundwater (Beeri & Phillips, 2007; Keddy et al., 2009). This region was formed after the last glacial maximum (Wisconsin) ∼12,000 years ago (Goldhaber et al., 2014). Wetlands in the PPR vary in size (<1 ha to >10 ha) and duration of flooding (from ephemeral to permanent), where medium sized wetlands (2–4 ha) have the highest CH_4 fluxes in this ecosystem (Bansal et al., 2023). This is in part due to these medium wetlands having longer hydroperiods relative to the smaller wetlands that become oxic as water evaporates and sediments are exposed. PPR wetlands are biogeochemical "hotspots" with a range of salinities and high levels of dissolved sulfur (pyritic sulfur, reduced organic sulfur, oxidized sulfur) (Zeng et al., 2013) resulting from groundwater flow through pyrite-rich glacial till (Van Stempvoort et al., 1994). Highlighting many of the uncertainties surrounding biogeochemical processes within these wetlands, high sulfate levels in the PPR have typically been attributed to lower CH_4 flux (Pennock et al., 2010). Recently we reported, however, simultaneously high levels of sulfate reduction and CH_4 flux in PPR wetlands in North Dakota (Dalcin Martins et al., 2017).

Biogeochemical processes in anaerobic wetland sediment are mediated, in part, by local redox conditions. The canonical redox ladder in wetland sediments predicts that diverse microbial metabolisms are governed by differences in the gain of free energy from reduction of terminal electron acceptors (TEAs) and proposes that nitrate reduction, iron reduction, sulfate reduction, and methanogenesis sequentially occur following the depletion of the most thermodynamically favorable TEA, dissolved oxygen (Burgin et al., 2011; Mobilian & Craft, 2022; Peiffer et al., 2021). Nevertheless, it has long been known that myriad physical and chemical factors can "bypass" this ladder, resulting in diverse microbial metabolisms occurring across small spatial scales (Chen et al., 2017). Sulfate reduction, a process often overlooked in freshwater systems, is thought to inhibit methanogenesis in high salinity environments by the activity of sulfate reducing bacteria which outcompete methanogens for hydrogen and acetate through higher free energy yields and therefore act as a thermodynamic control (Bartlett et al., 1987; Capone & Kiene, 1988; Hartman et al., 2024; Z. Wang et al., 1996). Numerous studies, however, have shown that sulfate reduction and methanogenesis can co-occur (Dalcin Martins et al., 2017; Schorn et al., 2022; Sela-Adler et al., 2017; Weston et al., 2011).

Methanogens produce CH_4 through three distinct pathways characterized by their substrate use: (a) hydrogenotrophic methanogenesis (reduce CO_2 using H_2, formate, ethanol, propanol, butanol), (b) acetoclastic methanogenesis (split acetate), or (c) methylotrophic methanogenesis (CH_3 groups cleaved from methanol or methylated amines, like trimethylamine; demethylating compounds including methoxylated substrates (e.g., aromatic methoxybenzoate), or methylated sulfur) (Angle et al., 2017; Kurth et al., 2020, 2021; Liu & Whitman, 2008; Narrowe et al., 2019). In freshwater wetlands, hydrogenotrophic and acetoclastic methanogenesis are often considered the dominant pathways contributing to methane production and are frequently the only pathways incorporated into process based ecosystem models such as *ecosys* (Grant, 1998; Grant et al., 2017). However, recent work across a range of freshwater and saline systems shows methylotrophic methanogenesis is a more active pathway than previously recognized (Ellenbogen et al., 2023; Narrowe et al., 2019; Tebbe et al., 2023; S. L. Tsola et al., 2024, 2021). Moreover, in many of these saturated systems methylotrophic methanogens have shown the ability to use "non-competitive" substrates (i.e., compounds only available to a particular functional guild of microorganisms such as methylotrophic methanogens), enabling co-occurrence of reductive microbial metabolisms that might otherwise be thermodynamically inhibited (Cozannet et al., 2023; King, 1984; Oremland et al., 1982; Schorn et al., 2022). Thus, the presence of non-competitive substrates can stimulate methylotrophic methanogenesis concurrently with sulfate-reduction.

While distinct redox zonation may occur across many meters in marine sediments (Jørgensen & Kasten, 2006), the abundance of organic inputs into PPR wetlands can drive multiple respiratory processes in surficial sediments, resulting in strong redox gradients over short length scales. Many previous studies in the PPR and elsewhere were performed at coarser scales (i.e., 3–10 cm) which has obscured the fine-scale spatial resolution needed to understand how biogeochemical processes interact in wetland environments (Angle et al., 2017; E. K. Bechtold et al., 2025; Dalcin Martins et al., 2017; He et al., 2015; Mondav et al., 2014). To better understand biogeochemical cycling and the factors mediating CH_4 production at the sediment-water interface, this study integrated geochemical profiling with microbial community analyses at a finer-scale spatial resolution (<1 cm) in surficial sediments from two distinct PPR wetlands, P7 and P8, at the Cottonwood Lakes study site in North Dakota. Although these two wetlands have some of the highest CH_4 fluxes and rates of sulfide reduction measured in terrestrial ecosystems (Dalcin Martins et al., 2017), historical data reveals six times greater annual CH_4 flux from P8 relative to P7 over a period of 19 years (Tangen & Bansal, 2019). This approach allowed us to directly link the presence of diverse electron acceptors with microbial communities to better understand the respiratory processes occurring along these wetland depth gradients. Moreover, results from this work offered new insights into the role of microbial communities and the corresponding geochemistry in mediating high CH_4 emissions from chemically distinct wetland sediments.

2. Methods

2.1. Site Description

The Cottonwood Lakes Study Area (47° 05′N: 99° 06′W) is a preserved research site operated by the United States Geological Survey (USGS) located northwest of Jamestown, North Dakota. The 92-ha site consists of 17 distinct wetlands with permanent-to-temporary inundation. Samples were collected from two permanent wetlands, P7 and P8 (Figure S1 in Supporting Information S1), which were chosen as study sites due to their historically high levels of CH_4 flux despite differences in wetland type and geochemistry (Bansal et al., 2016; Dalcin Martins et al., 2017). P7 is a permanent wetland categorized hydrologically as a "flow-through wetland" that is, groundwater moves through the wetland. Additionally, P7 is adjacent to agricultural fields and experiences nutrient-rich runoff resulting in algal growth. P8 is categorized as a "discharge wetland," receiving its water through groundwater flow from upland recharge and flow-through wetlands (Winter & Rosenberry, 1998). Thus, as groundwater flows through the environment, associated mineral dissolution results in much higher concentration of ions in discharge wetlands (Euliss et al., 2014; Seelig & DeKeyser, 2006). P8 is also characterized by dense cattail vegetation around the wetland perimeter and the resulting sediment is characterized by a thicker layer of surficial plant litter than seen in P7.

2.2. Sample Collection

Sediment cores were collected in triplicate from two locations in P7 wetland and one in P8 in October 2022 (Figure S1 in Supporting Information S1). Samples were collected in October because this is when flux is highest in many temperate freshwater wetlands (Delwiche et al., 2021). In P7, samples were collected from two distinct locations in order to understand spatial differences within the wetland. Site A was closer to the shore where the water column was shallower and there was more vegetation while site B was in the middle of the wetland with a deeper water column. P8 was sampled in one location in the middle of the wetland. At each sampling location cores were collected at least 1 m apart from each other to capture heterogeneity within each sampling location. Cores were collected using a modified Mooring System (Cataumet, MA) soil core to a depth of 15 cm in order to measure fine scale variability in microbiology and electrochemistry within the surficial sediments. After collection, cores were kept in capped core liners maintaining the water column over the sediment core to ensure in situ conditions in a vertical position, immediately put on ice and transported to the USGS facility in Jamestown where they were stored at 4°C until processing within 24 hr of collection. Microbiology analyses were performed on all cores and electrochemistry on two out of three cores from each site. An Ekman dredge was used to collect additional bulk samples on this date from P7 site A and P8 (near shore) wetlands for X-ray absorption near edge structure spectroscopy (XANES). These are bulk samples that average over the top 10 cm of the sediments. For this sampling, sediments were transferred to wide-mouth polypropylene centrifuge bottles within 5 min of collection, filled to the top with sediment to maintain redox conditions, stored on ice during transport from the field to University of Minnesota (24–48 hr), centrifuged to remove bulk water, and then stored at 4°C until processing for analysis.

2.3. Electrochemical Measurements

Electrochemical measurements were conducted the day after sediment cores were collected at the USGS facility. To allow microelectrodes to reach depths of up to 10 cm below the sediment-water interface (SWI), the cores were partially extruded, leaving 5 cm of overlying water above the sediment. Following partial extrusion, electrochemical measurements were conducted using a portable potentiostat (STAT-I 400s, Metrohm DropSense) and a three-electrode system, following the procedures in McAdams et al., 2016 (37). This system included a saturated Ag/AgCl reference electrode (BASi), a Pt-wire counter electrode (BASi), and either a gold-mercury (Au/Hg) amalgam (Luther et al., 2008; Ma et al., 2008) or a bismuth (Bi) film working electrode for high reduced sulfur cores (Waite et al., 2006).

Version of record at: https://doi.org/10.1029/ 2024JG008478

To initiate measurements, the reference and counter electrodes were positioned just above the SWI, while the working electrode was lowered from the surface of the overlying water to 10 cm below the SWI at intervals of 0.5–1 cm using a micromanipulator (Narishige). Initially, the Au/Hg electrode was employed to quantitatively measure dissolved O_2, Mn^{2+}, and Fe^{2+}, and qualitatively detect species like Fe^{3+}-organic compounds. It can also detect FeS, polysulfides, and free reduced sulfur ($\Sigma H_2S = H_2S + HS^- + S^{2-}$) up to several hundred micromolar (36). Cyclic voltammetry (CV) scans were conducted with scan rates of 1 V/s from −0.1 V to −1.8 V to −0.1 V (vs. Ag/AgCl). When the ΣH_2S peak began to interfere with other measurements, the Ag/Hg electrode was replaced with the Bi film electrode to prevent potential damage. Thus, the absence of electrochemical data in deeper sediments (>2 cm below the SWI) does not imply the absence of other species besides ΣH_2S but reflects analytical constraints. The Bi film electrode was specifically designed for the quantification of ΣH_2S at relatively high concentrations (mM levels). With this electrode, CV scans were performed at scan rates of 1 V/s from −1.6 V to −0.4 V to −1.6 V (vs. Ag/AgCl). All CV scans (by either Au/Hg or Bi film electrode) at discrete depths were repeated at least three times until no further changes were observed, and the final scan was analyzed. Electrochemical measurements were conducted on two out of three replicate cores, and the average and range of results from these two cores were plotted (Figure 1).

Both working electrodes, housed in polyether-ether-ketone (PEEK) tubing, were crafted, polished, and calibrated at the University of Delaware prior to the field campaign, following established protocols (McAdams et al., 2016). The Au/Hg amalgam working electrode underwent calibration with air, Fe^{2+}, and Mn^{2+} in a 20 mM NaCl solution under specified CV scan rates and ranges above. The peaks corresponding to dissolved O_2, Fe^{2+}, and Mn^{2+} were observed at potentials of approximately −0.32 V, −1.40 V, and −1.55 V (vs. Ag/AgCl), respectively. The current responses from cathodic CV scans using the Ag/Hg were analyzed quantitatively for O_2, Fe^{2+}, and Mn^{2+} based on calibration curves. Beyond the quantitative analyses, additional peaks corresponding to other redox species emerged during CV scans, depending on the cores and their depths. Three distinctive peaks were observed aside from those used in calibration: the peak at −0.6 V was consistently identified as ΣH_2S, −1.1 V corresponded to FeS, and another peak at −0.5 V was indicative of Fe(III)-organic complexes (Hakala et al., 2009; M. Hudson et al., 2022; Ma et al., 2008). The Bi film electrode was calibrated using HS^- in a 20 mM NaCl solution, with the peak for ΣH_2S detected at −0.6 V during anodic CV scans. Based on the established calibration curve, the current responses obtained with the Bi film electrode were exclusively analyzed for ΣH_2S and none of the other reduced forms of sulfur.

2.4. Porewater and Sediment Analyses

The sediment cores, initially partially extruded for electrochemical analyses, were further extruded using hydraulic pressure and sectioned into 1 cm intervals up to 10 cm depth using sterile spatulas. Every 1 cm, sediment discs were cut from the core, the outer portion was removed, and the remaining center was homogenized. The homogenized samples were collected into separate sterile DNase free tubes for geochemistry analysis and microbial community analysis, immediately placed on ice, and subsequently frozen until analysis.

Porewater extracted from sediments was analyzed for dissolved organic carbon (DOC), specific UV absorbance ($SUVA_{254}$), and total sulfur (S) concentration. Porewater was separated from sediment through centrifugation at 1,000 g for 10 min. 4-mL of each porewater sample was diluted fivefold with ultrapure water and split into two portions for DOC measurements using a TOC-L (Shimadzu, Kyoto, Japan) and total S measurements using an ICP-OES at the University of Delaware Core Laboratory for Soil, Plant and Water Analysis. The remaining undiluted porewater samples were directly assessed for absorbance at 254 nm using a UV-vis spectrophotometer (Agilent Cary 60, Santa Clara, CA). From these measurements, $SUVA_{254}$ ($L \cdot mg\ C^{-1}\ m^{-1}$) was calculated as the ratio of the absorbance at 254 nm (cm^{-1}) to DOC concentration ($mg\ C \cdot L^{-1}$).

pH was measured using a modified protocol from Trimarco et al. (2023). In brief, sediment was combined with molecular-grade water in a 1:4 ratio. Soil slurries were then vortexed for 15 s, placed on a shaker at 120 RPM at 20°C for 1 hr, and centrifuged at 7,000 g for 10 min before the supernatant was transferred to a sterile tube and pH was read using a pH electrode.

2.5. X-Ray Absorption Spectroscopy

Iron and S speciation in sediments collected via Ekman dredge was measured by bulk synchrotron X-ray absorption near edge structure (XANES) spectroscopy. Moist sediments were prepared in a H_2/N_2 (g)-filled Coy

AGU ADVANCING EARTH AND SPACE SCIENCES

Journal of Geophysical Research: Biogeosciences 10.1029/2024JG008478

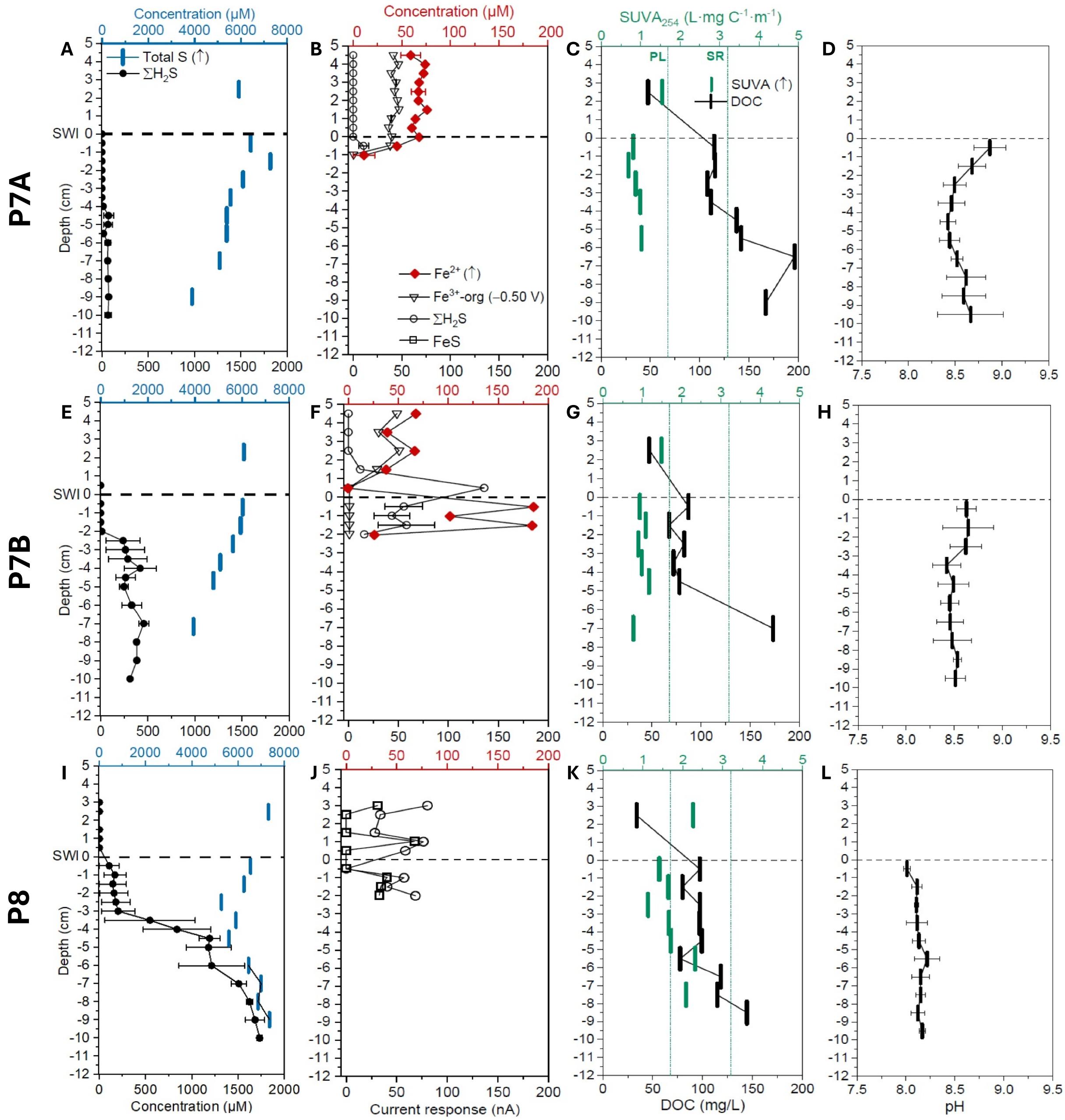

Figure 1. On-site electrochemistry data including ΣH_2S concentrations (bottom *x*-axis of panels a, e, i), Fe^{2+} concentrations (top *x*-axis of panels b, f, j), and current responses for ΣH_2S, Fe^{3+}-organic complexes (Fe^{3+}-org), and FeS (bottom *x*-axis of panels B, F, and J) at different depths of cores P7A (a–d), P7B (e–h), and P8 (i–l). Total S concentration, DOC, $SUVA_{254}$, and pH of overlying water and porewater are plotted against the top *x*-axis of panels (a, e, i); the bottom *x*-axis of panels (c, g, k); the top *x*-axis of panels (c, g, k); and the bottom *x*-axis of panels (d, h, l), respectively. Horizontal reference lines at 0 cm depth represent the sediment-water interface (SWI). Two vertical reference lines at 1.7 and 3.2 $L{\cdot}mg\ C^{-1}\ m^{-1}$ in panels (c, g, k) are the $SUVA_{254}$ of Pony Lake (PL) fulvic acid and Suwannee River (SR) fulvic acid, respectively.

anaerobic chamber (Coy Laboratory Products). A slurry was prepared with deoxygenated water, applied by pipet to polyethersulfone (PES) membrane filters (0.2 µm, 47 mm, Fisher Scientific), and dried by evaporation and wicking of water (Kimwipes) for 1 hour. For Fe XANES, each PES filter was sealed between two pieces of Kapton adhesive. For S XANES, the dried sample was removed from the PES filter with a micro-spatula and applied to double-sided adhesive. All samples were sealed in mylar pouches (Sorbent Systems) to protect them from the ambient atmosphere during transportation to the beamline. Iron XANES spectra were acquired on the QAS beamline, National Synchrotron Light Source II, in fluorescence and transmission modes using an Fe foil for

Version of record at: https://doi.org/10.1029/ 2024JG008478

monochromator calibration. Sulfur XANES spectra were collected at the SXRMB beamline, Canadian Light Source, in fluorescence and totally electron yield modes using a powdered gypsum ($CaSO_4$) for monochromator calibration. For both beamlines, samples were protected from the ambient atmosphere before and during analysis. For all XANES data, repeat scans were checked for photon damage (none observed). Average of scans, monochromator energy calibration, pre-edge subtraction, and post-edge normalization were performed in *Athena* software (Ravel & Newville, 2005). Linear combination fitting (LCF) was performed using LabView software (Marcus et al., 2004) using previously characterized and published reference databases (Cron et al., 2020; Marcus et al., 2008) and published methods (Manceau et al., 2002; Pierce et al., 2022; Stewart et al., 2021).

2.6. DNA Extraction, 16S rRNA Gene Sequencing, and qPCR

DNA was extracted from depth-resolved sediments using Zymo Research Quick-DNA™ Fecal/Soil Microbe Microprep Kit, following the manufacturer's protocol. Amplicon libraries were prepared using a single step PCR to amplify the V4 region of the 16S rRNA gene with the primers 515F/806R (Apprill et al., 2015; Parada et al., 2016) following the Earth Microbiome Project (EMP) PCR protocol. SequalPrep Normalization Kits (ThermoFisher) were used to cleanup and standardize concentrations of each PCR product. Pooled DNA products were sequenced on the Illumina MiSeq Platform using 251 bp paired-end sequencing chemistry at the Microbial Community Sequencing Lab (University of Colorado Boulder).

Sequence reads were processed using QIIME 2 (v2021.2). Samples were demultiplexed, forward and reverse reads were trimmed to 230 bp, paired end reads were then merged and binned inferring amplicon sequence variants (ASVs). Taxonomic identities were assigned using the naïve Bayes sklearn classifier with the Silva 138 database (Quast et al., 2013) and GTDB-Tk database (v2.1.1 r207) (Chaumeil et al., 2020). The data from this study contained 45,462 ASVs from 90 samples. After filtering out chloroplast and mitochondria, resulting reads ranged from 6,827 to 29,839 per sample. Alpha and beta diversity analyses were conducted on samples rarefied to 10,000 reads, which resulted in the loss of three samples due to low read depth. Taxonomic analyses were conducted on unrarefied samples.

Microbial DNA samples corresponding to each sediment fraction were used to quantify the *mcrA* gene using qPCR of *mcrA* as a proxy for the abundance of methanogens per gram of sediment. All samples were amplified in triplicate using the mlas-F (5′ GGT GGT GTM GGD TTC ACM CAR TA 3′) and mcrA-R (5′ CGT TCA TBG CGT AGT TVG GRT AGTGA 3′) (Narihiro & Sekiguchi, 2011) primers. Reactions were set up using Luna Universal qPCR mastermix (NEB, Ipswich, MA, USA) following the manufacturer protocol. The abundance of *mcrA* was compared to methanogen relative abundance data from 16S rRNA gene sequencing to understand the abundance of methanogens from each pathway.

2.7. Functional Annotation

To move beyond community composition and understand functional profiles of the microbes found in our samples, ASVs were compared to metagenome assembled genomes (MAGs) from the Multiomics for Understanding Climate Change (MUCC) v 2.0.0 database (E. Bechtold et al., 2024; E. K. Bechtold et al., 2025). MUCC is a publicly available database of metagenomes, metatranscriptomes, and amplicon data collected from freshwater wetlands. This database contains 3,634 high and medium quality, dereplicated (99% genome identity) MAGs recovered from a range of freshwater saturated sediments (including 333 from PPR). Previous research has shown that 16S rRNA gene data can be connected to ecosystem relevant MAG databases resulting in trends in functional profiles. Metagenomics is often prohibitive in many studies due to cost and computational resources. 16S rRNA gene data is cheaper and more high-throughput, allowing for greater sampling efforts and replication. By building publicly available ecosystem databases, some functional profiles of microbial communities can be inferred from the 16S rRNA gene profiles. However, this method is not a comprehensive assessment of the functional profile of a community because it is unlikely that every taxa identified using 16S rRNA gene analysis will have a MAG representative in the ecosystem database, especially in diverse systems like wetland sediments. Additionally, because of heterogeneity across taxa, it is critical to use ecosystem specific databases because the genomic and functional profiles of taxa can vary between different ecosystems. In our study, only 16S rRNA gene data was generated for the samples collected. These samples were then compared to the MUCC v2.0.0 database (E. Bechtold et al., 2024) following the previously published methods in which taxa identified via 16S rRNA genes are compared to the MAG database at the genus level (E. K. Bechtold et al., 2025). The PPR MAGs are from previous studies (E. K. Bechtold et al., 2025; Dalcin Martins et al., 2017) and new metagenomes were not analyzed from the sediment collected in this study. Utilizing this database to link 16S rRNA gene sequencing to genomes from relevant wetland lineages enables more accurate functional prediction of amplicon data. MAGs from the MUCC database were assigned taxonomy using GTDB-Tk (v2.1.1 r207) (Chaumeil et al., 2020) and were annotated using DRAM (v1.4.4) (Shaffer et al., 2020). Using DRAM outputs, MAGs were assessed to understand metabolic capabilities of the organisms, specifically for metabolisms including methanogenesis, methanotrophy, sulfur reduction, sulfur oxidation, iron reduction, denitrification, DNRA, and fermentation (Oliverio et al., 2024). Methanogens and methanotrophs were first assigned to all 16S rRNA taxa based on taxonomy following previously published criteria (E. K. Bechtold et al., 2025). If those taxa contained a representative MAG in the MUCC database then the methanogenic pathway was characterized as outlined in Ellenbogen et al. (2023). If the taxa did not have a MAG representative, then the appropriate pathway was assigned using published literature (Table S4 in Supporting Information S1).

Additionally, specific genomes were annotated to determine if they encoded hydrogenases. Hydrogenase presence was determined using DRAM if subunit completion of multi subunit hydrogenases existed. Additionally, all PPR MAGs were searched for arylsulfatase genes using BLAST-X with a FASTA reference file of the arylsulfatase AtsA from *Pseudoalteromonas carrageenovora* (Barbeyron et al., 1995; Stam et al., 2023). The BLAST-X output was filtered to only include MAGs with a bitscore >60. All MAGs, their DRAM annotations, and a curated list of methanogens and methanotrophs can be found at https://doi.org/10.5281/zenodo.14532347 (E. Bechtold et al., 2024).

2.8. Statistical Analyses

Differences in alpha diversity (Shannon Diversity Index and observed species richness (number of ASVs)), relative abundance of taxonomic and functional groups (from qPCR and MAGs), and pH both across sample locations and depths within samples were determined using analysis of variance (ANOVA) followed by Tukey HSD tests as implemented in R Studio (Wickham, 2016). Linear models were used to assess if relative abundance of Desulfobacteria was predictive of H_2S levels, depth, and their interaction within each wetland along the depth gradient using the *lm* function followed by model selection using Akaike's Information Criterion (AIC) and a regression model conducted using *ggpubr* in R (Kassambara, 2023). Permutational analysis of variance (PERMANOVA) using Bray-Curtis distances was conducted to determine if community differences existed between sites and based on sampling depth. Results were visualized using non-metric multidimensional scaling (NMDS). PERMANOVA and NMDS were conducted using the vegan package (Oksanen et al., 2019) and visualized using *ggplot2* (Wickham, 2016). P values from ANOVA and PERMANOVA analyses were adjusted for multiple comparisons using the Benjamini & Hochberg method (Benjamini & Hochberg, 1995).

3. Results

3.1. Distinct Wetland Hydrology and Chemistry Is Reflected in Variable Microbial Community Composition

Depth profiles of sedimentary porewater chemistry from each site were characterized using on-site electrochemical measurements, supplemented by off-site (at the University of Delaware) analysis of extracted porewater for total S, DOC, total $SUVA_{254}$, and pH (Figure 1). Although distinct profiles emerged between the cores, reduced free sulfur (ΣH_2S) was observed in sediment porewater across all three locations (Figures 1a, 1e, and 1i), with concentrations increasing with depth. These porewaters also exhibited elevated total S concentrations (4–8 mM), high DOC concentration (50–200 mg/L), and low $SUVA_{254}$ (≤ 2 L·mg C^{-1} m^{-1}) (Chin et al., 2023). $SUVA_{254}$ is a measure of the aromatic content of dissolved organic matter (DOM) in porewaters, with higher values indicating greater aromaticity. Most $SUVA_{254}$ values at this site were lower than that of the microbial end member Pony Lake (PL) fulvic acid (1.7 mg C^{-1} m^{-1}), with a few values in P8 falling between the PL fulvic acid and the terrestrial end member Suwannee River (SR) fulvic acid (3.2 L·mg C^{-1} m^{-1}). The very low $SUVA_{254}$ values observed at this site suggest that the DOM is of low overall aromaticity and highlights the unique composition of DOM at this site.

Notable differences in ΣH_2S concentrations were observed: Within wetland P7, P7A exhibited concentrations below 100 μM, whereas P7B contained ΣH_2S concentrations as high as 500 μM. Wetland P8 showed markedly higher ΣH_2S levels, as also noted in prior studies at this site (McAdams et al., 2016; Pennock et al., 2010). In P8,

ΣH_2S first appeared in shallow sediment depths (0–3 cm) and increased to 1,750 μM in deeper sediments. The higher concentrations and presence of ΣH_2S at shallower depths led to the detection of FeS in P8 (Figure 1j), whereas in P7, only free Fe^{2+} and Fe^{3+}-organic complexes were detected (Figures 1b, 1f, and 1j). Additionally, P8 was distinguished by slightly lower pH values (Figures 1d, 1h, and 1l). Considering that the pH of these porewaters ranged between 8 and 9 at all locations and knowing that the first pK_a of H_2S is around 7, it is likely that ΣH_2S was predominately present as HS^-.

XANES analysis revealed that secondary 2:1 phyllosilicate minerals dominated Fe speciation in both P7 and P8 wetlands in the top 10 cm of sediment (~75 mol%; Table S1 in Supporting Information S1). The remainder of Fe was in the form of primary silicates. No Fe-bearing sulfide minerals were detected by bulk Fe XANES analysis. Sulfur speciation for P8 sediments was 75 mol% organic forms (organic monosulfide and ester sulfate; Table S2 in Supporting Information S1) with 4 mol% Fe monosulfide (mackinawite, $Fe_{(1+x)}S$ $x = 0$–0.11). In contrast, P7 sediments had 31 mol% organic sulfur species and 57 mol% Fe sulfide (greigite, Fe_2S_4; Table S2 in Supporting Information S1). The best fits to S XANES data for both P7 and P8 sediments included ~10–20 mol% reference spectra having disulfide or S-S bonds. In database sensitivity testing, both elemental S (only S-S bonds) and cystine (R-S-S-R′) provided equally good fits to the data, but the disulfide bonds in the pyrite (FeS_2) reference spectrum did not provide a good fit based on the normalized sum of square parameter. Overall, the majority of Fe in the sediments was in the form of 2:1 phyllosilicates while organic forms were more important for S speciation. While the sediments and porewaters are rich in both Fe and S, Fe-S minerals were detected in relatively low abundance and organic forms of S were abundant, especially in P8.

Microbial communities were sampled at high resolution by sectioning cores every 1 cm, allowing for direct comparisons to the electrochemistry and geochemistry measurements. Alpha diversity, measured using richness, was not significantly different based on site or sample depth but was different based on sampling location. P7A, which was sampled closer to shore, was significantly different from P7B ($p = 0.04$) and P8 ($p = 0.02$) which were both sampled in the middle of the wetlands in deeper water (Figures 2a–2c). Clear community trends were observed across core depths and sites. Using a PERMANOVA to test statistical differences and an NMDS to visualize communities, we found that community beta diversity in P7A and P7B were significantly different from each other ($R^2 = 0.08$, $F = 5.08$, $p = 0.014$), but that P7A ($R^2 = 0.55$, $F = 70.06$, $p < 0.001$) and P7B ($R^2 = 0.48$, $F = 53.51$, $p < 0.001$) were even more different from P8 than from each other (Figure 2d), thus indicating that heterogeneity is greater between wetlands despite spatial heterogeneity being present within a given wetland. Additionally, within each site we observed changes in microbial communities that corresponded with sediment depth and corresponding variability in pore water chemistry (Table S3 in Supporting Information S1).

3.2. Abundant and Diverse Fermenters Likely Support Respiratory Metabolisms

The MUCC v2.0.0 database is a publicly available database composed of metagenomes, metatranscriptomes, and amplicon data gathered from freshwater wetlands (E. Bechtold et al., 2024). Previous research using this database showed that you can link environmentally relevant metagenome assembled genome (MAG) data to 16S rRNA amplicon data, allowing for trends in functional potential of microbial communities to be linked with geochemical processes (E. K. Bechtold et al., 2025). Metagenomic sampling is both computationally and cost expensive, and can require high sequencing depth to capture community taxonomic diversity comparable to that identified through 16S rRNA amplicon sequencing. By building ecosystem specific databases, functional information can be linked to amplicon data, allowing for functional predictions of microbial communities in that ecosystem. Using this database and previously published methods, MUCC was used to link ASVs from 16S rRNA gene sequencing with metagenome assembled genomes (MAGs) from temperate freshwater wetland environments. MUCC is a comprehensive resource of MAGs assembled from freshwater wetland samples that reduces the need for extensive metagenomic sampling. We characterized the microbial community using 16S rRNA gene data and identified which taxa matched genomes in the MUCC database. All data and relative abundances presented are derived from 16S rRNA profiles, while functional profiling is based on the genomes from the MUCC database that correspond to the matched 16S rRNA taxa. Using MUCC we were able to identify diverse anaerobic respiratory processes both across sites and sediment depth profiles. E2 (Phylum Thermoplasmatota), an archeal class composed of the genus SM-150, demonstrated a significantly higher relative abundance in P8 compared to P7 ($p < 0.001$). Additionally, taxa affiliated with the SM-150 genus displayed a depth-dependent decrease in relative abundance in P8 that was also significantly correlated with ΣH_2S (Figure S2 in Supporting Information S1), while no depth or ΣH_2S trend was observed in either of the P7 sites (Figures 3b, 3e, and 3h). Through genus level

Journal of Geophysical Research: Biogeosciences 10.1029/2024JG008478

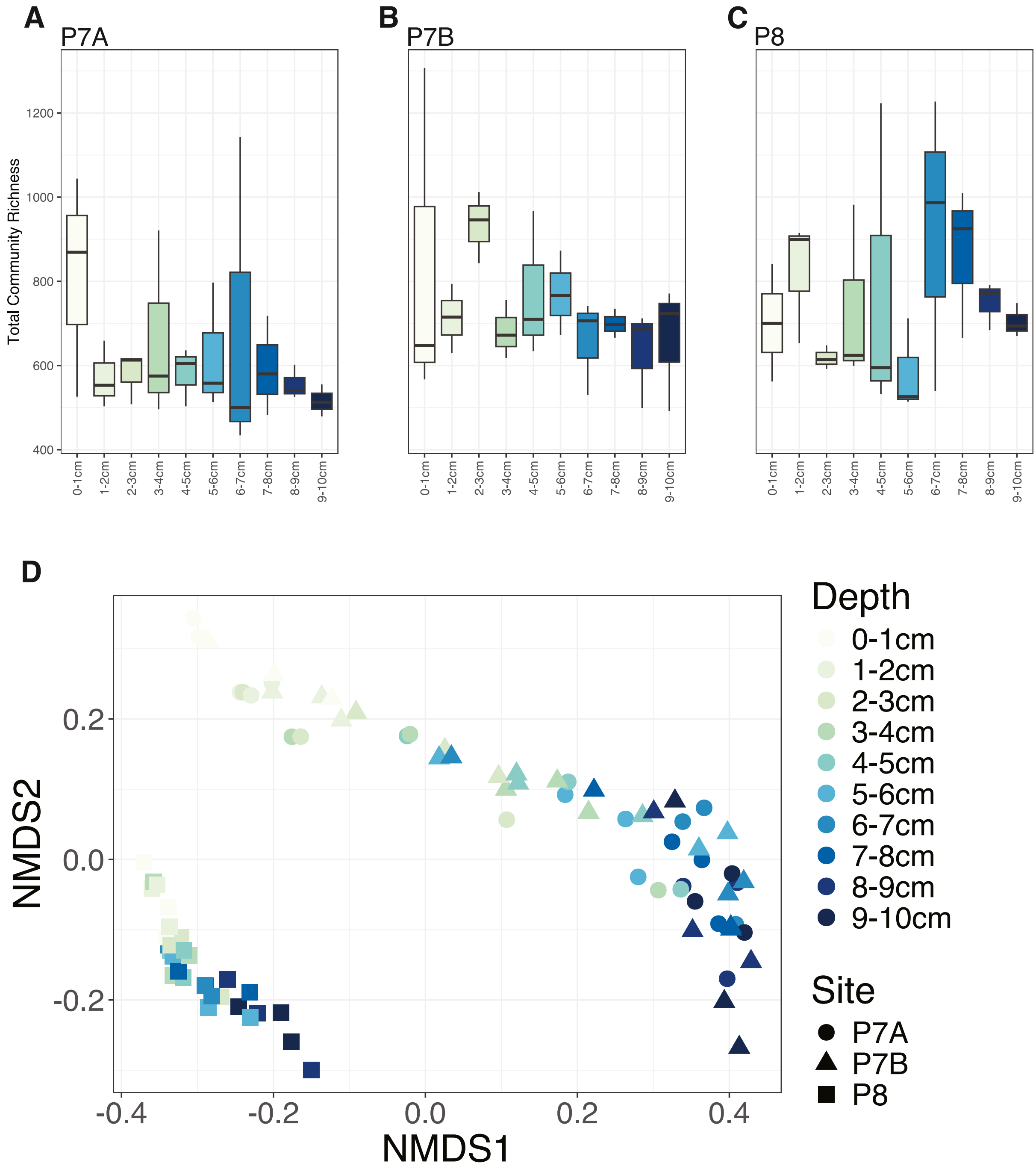

Figure 2. Alpha diversity, measured using species richness across a depth gradient, in P7A (a), P7B (b), and P8 (c) shows no distinct trends based on depth or site. (d) NMDS shows community composition has distinct trends between wetlands and based on depth but shows only small differences within wetland sampling sites. Sediment depth is given based on color while wetland site is shown by different shapes.

identification, we associated SM-150 with 7 unique MAGs in the MUCC database. Subsequent analysis using DRAM annotations of representative genomes revealed that SM-150 are likely obligate fermenters, requiring anaerobic conditions and utilizing organic compounds as terminal electron acceptors.

Anaerolinea (Phylum Chloroflexota), one of the two most abundant classes of microbes within the samples analyzed here, constituted approximately 20% of the communities across both sites. Within the *Anaerolinea* class,

Version of record at: https://doi.org/10.1029/ 2024JG008478

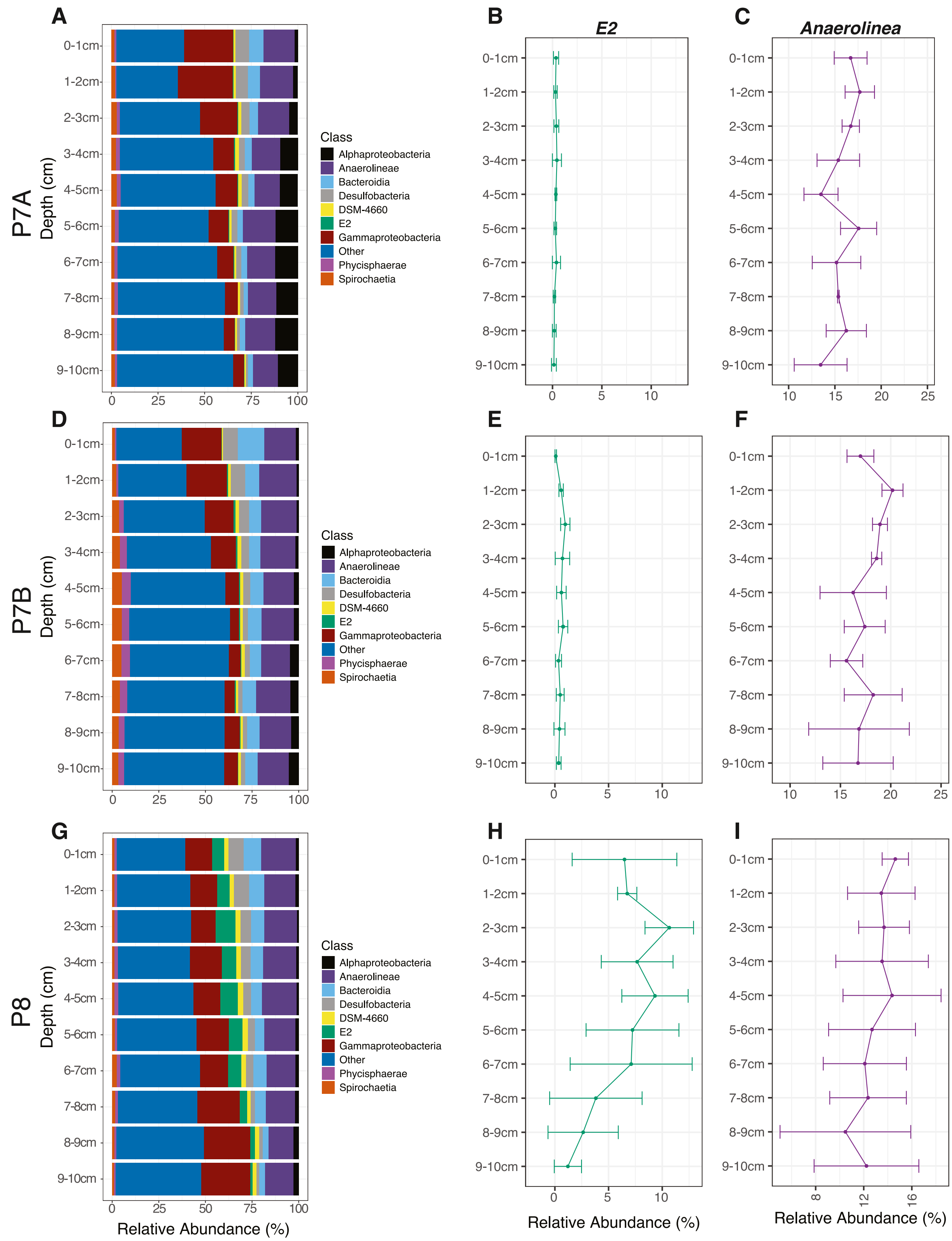

Figure 3. Taxa barplots of the most abundant microbial classes (a, d, g) show trends exist over depth and between wetlands. Class E2 composed entirely of an obligate fermenter from the genus *SM-150* had significantly higher abundance in P8 (h) compared to P7A (b) and P7B (e). The class Anaerolinea makes up a large portion of the communities in P7A (c), P7B (f), and P8 (i) but its relative abundances are not different between sites or along the depth gradient.

four families (*Anaerolineacea, ENVOPs12, JAAYZQ01, UBA4823*) made up a substantial portion of the community with relative abundances found over 2% across both sites (Figures 3c, 3f, and 3i; Figure S3 in Supporting Information S1). *Anaerolineacea* matched with 7 unique MAGs from the MUCC database that encoded functional potential for either iron-reduction or fermentation. *ENVOPs12* matched with 47 unique MAGs encoding a wide range of metabolic capabilities including iron reduction, sulfate reduction, thiosulfate reduction, denitrification, DNRA, and fermentation. *JAAYZQ01* matched with 11 unique MAGs encoding metabolisms capable of iron reduction, denitrification, DNRA, and fermentation while *UBA4823* matched with 41 unique MAGs encoding genes for iron reduction, thiosulfate reduction, denitrification, and DNRA. Given the reducing conditions within PPR sediments, this diverse functional potential may account for the high relative abundance of the *Anaerolinea* class in this ecosystem.

3.3. Sulfur Species Represent Key Sources of Electron Donors and Acceptors Throughout the Sediment Profile

Putative sulfate reducing bacteria (SRB) (from the Phyla Desulfobacterota, Desulfobacterota B, Desulfobacterota C, Desulfobacterota E, Desulfobacterota G, and Desulfobacterota I) constituted a substantial proportion of the microbial communities throughout the entire depth profile in both P7 and P8 wetlands (Figures 4a, 4d, 4g and Figure S4 in Supporting Information S1). These SRB had significantly higher relative abundances in P8 compared to P7 ($p < 0.001$). In P7, SRB relative abundances significantly decreased with depth ($p < 0.001$), while no significant depth trend was observed in P8. Within these phyla, 8 bacterial classes were identified at high relative abundance (>2% within a site) (Figure S4 in Supporting Information S1). Taxa affiliated with Desulfobaccia, DSM-4460, Syntrophia and Syntrophobacteria exhibited similar trends between sites: their relative abundances were generally consistent throughout the depth profile (∼2–4% relative abundance). In contrast, taxa affiliated with Dehaloccoidia and BSN033 were present at increasing relative abundances with depth in both P7 and P8, with a stronger upward trend in P8. Finally, taxa affiliated with Binatia had lower relative abundances in P8 relative to P7. While these taxa displayed no depth trend in P8, their relative abundances increased with depth in P7.

Desulfobacteria was the most abundant putative SRB across both sites, with average relative abundances at 7.3% (P7A), 7.5% (P7B), and 8% (P8) at the sediment-water interface (top 1-cm of sediment). At deeper depths however (3–10 cm) these taxa displayed consistent depth-dependent decreases in relative abundance across the sites. When plotted against H_2S concentrations, Desulfobacteria relative abundances displayed a strong negative correlation within the sediment profiles (Figures 4c, 4f, and 4i). In both P7 and P8, AIC-based model selection identified the model including an interaction between H_2S and depth as the best predictor of *Desulfobacteria* abundance, indicating a relationship between H_2S and *Desulfobacteria* varies with depth rather than being solely confounded by it. Desulfobacteria MAGs from genus SpSt-50, a dominant Desulfobacteria in these communities, encoded both [NiFe] and [FeFe] hydrogenases and thus are likely highly versatile in their ability to use H_2, likely increasing their competitive advantage over hydrogenotrophic methanogens.

Given the high presence of ester-sulfate compounds identified through XANES, the functional potential for processing of ester-sulfate compounds was assessed within PPR MAGs from the MUCC database, revealing genes encoding arylsulfatases across a range of SRB affiliated with the phyla Desulfobacterota. 14 MAGs from the classes BSN033, Desulfobacteria, DSM-4660, DSWW01, and Syntrophia contained the enzymes, with five unique genera from the Desulfobacteria class encoding arylsulfatases, including SpSt-50. An additional 72 MAGs from 24 different bacterial Classes contained arylsulfatases demonstrating the widespread occurrence of sulfation functionality in the PPR sediment microbial community.

In addition to high prevalence of SRB, putative sulfur oxidizers also comprised a large part of the communities. The genus *Thiobacillus* exhibited significantly higher relative abundances in P8 compared to P7($P < 0.001$). The genus was composed of two species: *Thiobacillus denitrificans B* dominated both sites while *Thiobacillus thioparus* was present but at lower levels in P7 and P8. Across P7 subsites, *Thiobacillus* displayed the highest relative abundances in surface sediment layers, significantly decreasing with sediment depth until it was absent in the deeper layers (P7A: $R^2 = 0.94$, $P < 0.001$; P7B: $R^2 = 0.9$, $P < 0.001$) (Figures 4b and 4e). In P8 however, *Thiobacillus* relative abundances were consistently above 5% and significantly increased with depth ($R^2 = -0.93$, $P < 0.001$) where there were also higher levels of H_2S (Figure 4h).

Version of record at: https://doi.org/10.1029/ 2024JG008478

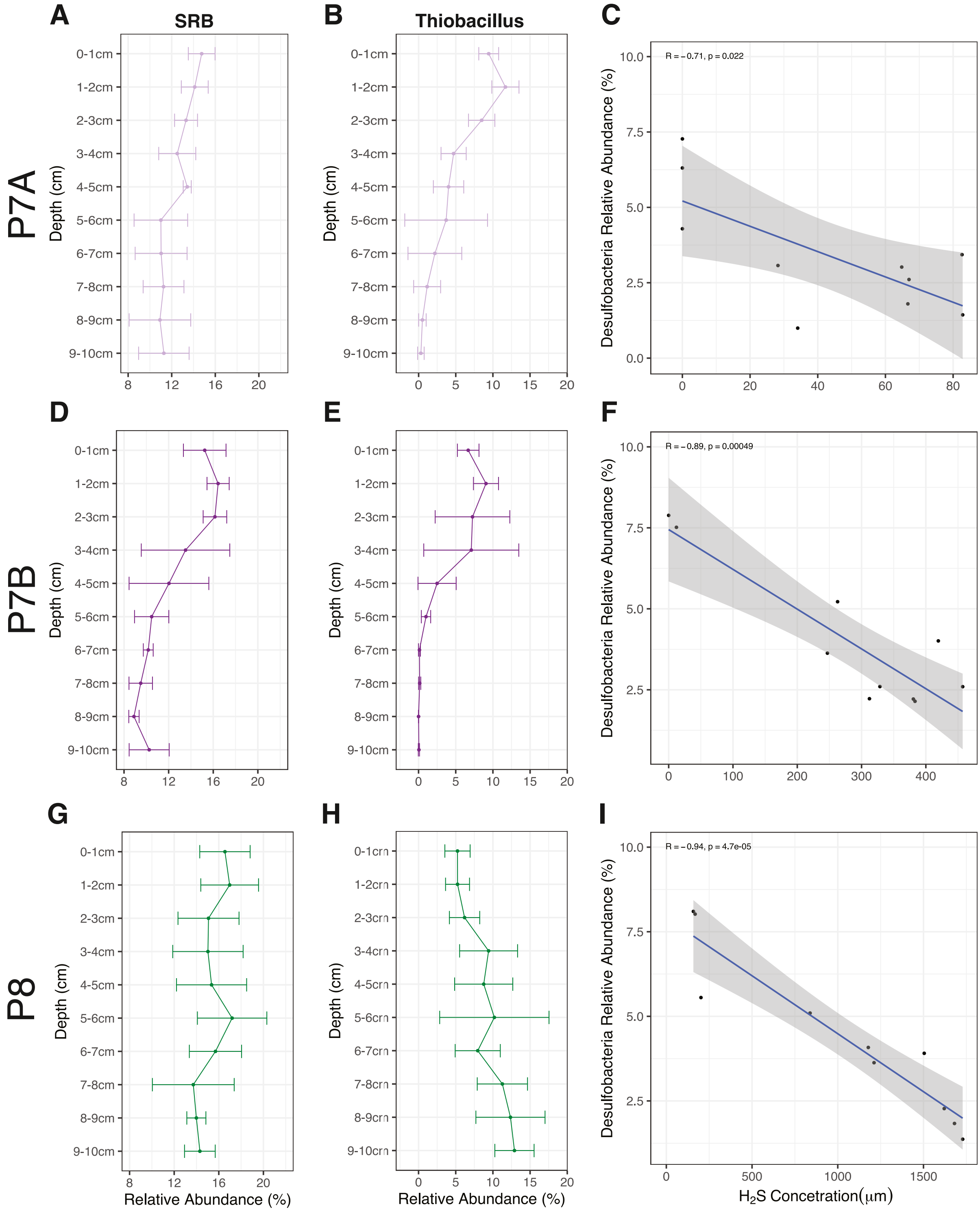

Figure 4. Sulfur cycling microorganisms make up a substantial proportion of the communities in P7A (a–c), P7B (d–f), and in P8 (g–i). Sulfate reducing bacteria (SRB) are found at high relative abundances across sites and depths (a, d, g). Thiobacillus, a sulfur-oxidizing bacteria, was found in high abundance across sites demonstrating its importance in sulfur cycling in PPR. P7A (b) and P7B (e) showed higher relative abundance in the surface sediments whereas P8 (h) had higher abundance showed a slight increase over depth. The relative abundance of the class Desulfobacteria, one of the dominant groups of SRB found in PPR, was significantly correlated with the concentration of ΣH_2S found in each site. Stronger correlations, given by R values closer to -1 and lower p values, were found as H_2S levels increased within sites.

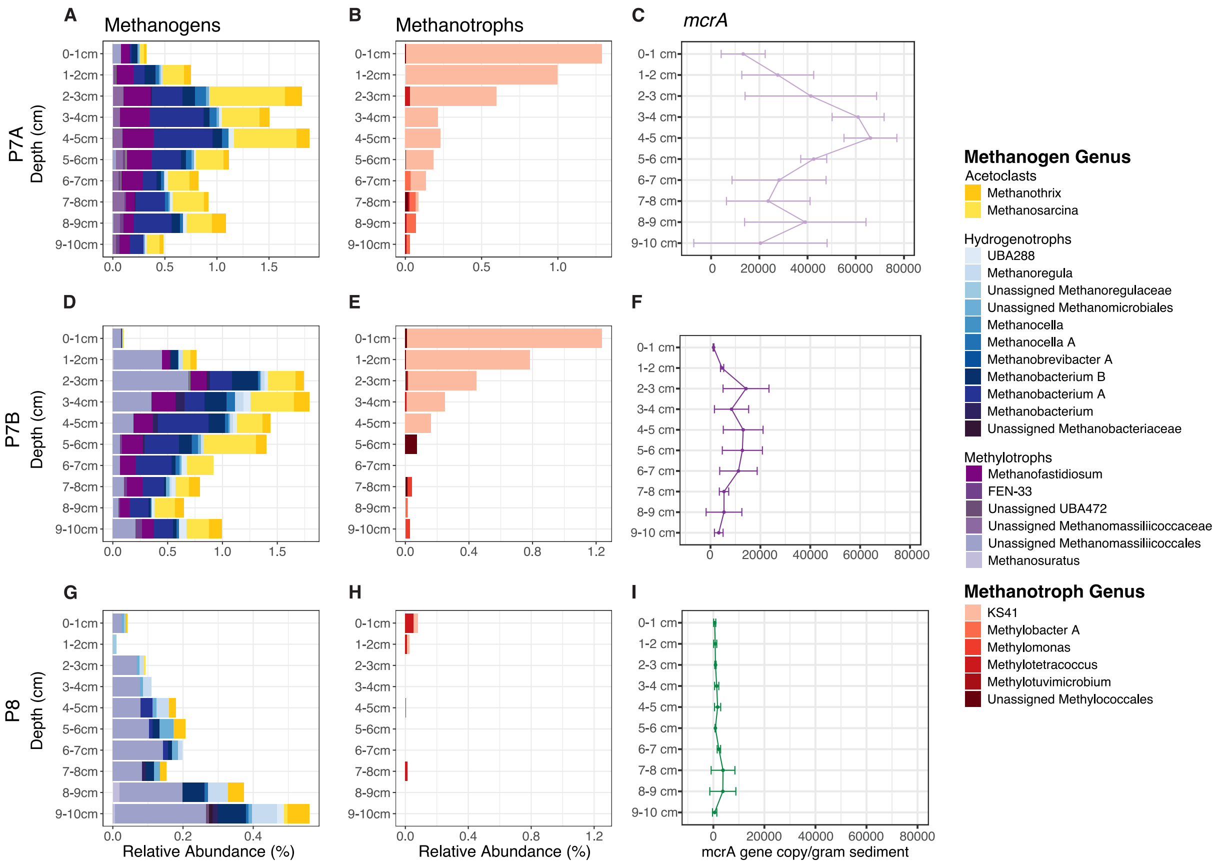

Figure 5. Methanogen (a, d, g) and methanotroph (b, e, h) relative abundance was calculated for each site across the depth gradient. Additionally, methanogenic pathways are shown. Acetoclastic methanogens are represented in yellow, hydrogenotrophic methanogens in blue, and methylotrophic methanogens in purple. (c, f, i) The abundance of mcrA gene was calculated using qPCR of the *mcrA* gene normalized as counts per gram of soil extracted to compare how relative abundance of methanogens compared to abundance of the *mcrA* marker gene in P7A (c), P7B (f), and P8 (i).

3.4. Distinct CH_4-Cycling Microbes Differentiate Communities Between Prairie Pothole Wetland Sites

Distinct differences in dominant methanogenesis pathways were found between P7 and P8 wetlands, although conserved patterns persisted in the P7 subsites. In P7, all three methanogenesis pathways were represented at each subsite, with acetoclastic methanogens the most abundant in P7A and putative methylotrophic methanogens the most abundant in P7B (5A, 5D, 5G). Depth-related trends observed across P7 subsites showed a minimal presence at the sediment surface (0–1 cm), a subsequent increase in relative abundances at 2–5 cm, followed by a decline. These trends mostly aligned with qPCR data of the *mcrA* gene with a few exceptions, demonstrating a spike and subsequent decline in *mcrA* abundance (Figures 5c and 5f). Wetland P8 hosted a distinct methanogen community, dominated by methylotrophic methanogens from the order *Methanomassiliicoccales* that increased in both relative abundance and abundance of *mcrA* with depth. Although *mcrA* abundance showed a decline at 9–10 cm while the relative abundance of inferred methanogens increased, these discrepancies could result from a variety of factors including differences in microbial biomass and varying numbers of *mcrA* and 16S rRNA gene copy numbers. In contrast, acetoclastic methanogens were either entirely absent in certain samples or, when present, were found in extremely low relative abundances (Figure 5g). Furthermore, sediments from wetland P8 displayed significantly lower overall methanogen abundance compared to P7A ($p < 0.001$) and P7B ($p = 0.009$) (Figures 5c, 5f, and 5i).

In both P7 and P8, the methanotroph community, as determined from the 16S rRNA gene sequencing profile, exclusively consisted of aerobic methanotrophs (Figures 5b, 5e, and 5h). Within the P7 subsites, a consistent pattern emerged where genus *KS41* dominated the methanotrophic community in the top 5 cm of sediment. Deeper subsections in P7A were characterized by the genus *Methylobacter A*, while P7B exhibited dominance of

Version of record at: https://doi.org/10.1029/ 2024JG008478

the genus *Methylomonas*. Notably, both P7 subsites displayed a similar relative abundance of methanotrophs, with the highest values in the top sediment layers that then decreased with depth. Conversely, P8 displayed a comparable decreasing trend, but methanotrophs composed a significantly smaller proportion of the community compared to P7 ($p < 0.001$) and were dominated by *Methylotetracoccus* and *KS41*. Additionally, methanotrophs were distributed across all sediment layers in P7, whereas they were nearly absent below the top 2 cm in P8.

4. Discussion

In these wetland sediments, differences in sediment biogeochemistry were measured within P7 across two distinct sampling locations, likely arising from factors including water column depth, inputs of organic material from nearby plants and their root exudates, and oxygen concentrations (Arnold et al., 2023). However, combined chemical and microbial analyses revealed that differences *between* wetlands were significantly greater than these *within*-wetland differences. Thus, while the research described in this paper focuses on inter-wetland biogeochemistry and microbiology, future work is needed to fully understand how these same processes vary and influence CH_4 flux across small spatial scales within individual wetlands.

The wetlands studied in this work have high concentrations of DOC (50–200 mg/L, Figure 1) resulting in high rates of microbial metabolism and the rapid onset of anoxia at the sediment-water interface, as evidenced by the presence of sulfate reducers and methanogens co-occurring in surficial sediments (Dalcin Martins et al., 2017). Sulfate concentrations are generally low in freshwater wetlands, but pore waters in the flow-through and discharge wetlands at the PPR complex can receive elevated sulfate concentrations (with a total S concentration of 4–8 mM, Figure 1) from hydrologic connectivity with groundwater circulating through pyrite-containing glacial till (Van Stempvoort et al., 1994; Zeng et al., 2013). Electrochemical measurements revealed high concentrations of ΣH_2S in P8, with levels increasing with depth across all wetland locations. These patterns highlight the importance of sulfate reduction in driving carbon mineralization in these sediments and align with previous measurements of high sulfate reduction rates in this system (Dalcin Martins et al., 2017).

The cycling of oxidized and reduced sulfur species in these wetlands is strongly influenced by local redox conditions, iron availability, and microbial community composition, which together shape distinct sulfur cycling dynamics between sites. Based on our measurements, we infer that any aqueous sulfate derived from pyrite weathering is rapidly consumed by sulfate-reducing bacteria (SRB), with the resulting ΣH_2S reacting with abundant pore water DOC to form either organic monosulfides or ester-sulfates, depending on the redox state of the DOC (as indicated by XANES data). In wetland P7, the inferred higher concentrations of ferrous iron in pore water promoted the precipitation of abundant iron sulfide minerals, particularly greigite, in surficial sediments. P7 also exhibited lower relative abundances of putative sulfur-oxidizing *Thiobacillus* species which decreased with depth, suggesting that the sequestration of ΣH_2S in Fe-sulfide phases may limit this metabolism (Gramp et al., 2010). In contrast, P8 had significantly higher concentrations of ΣH_2S and correspondingly higher *Thiobacillus* relative abundances which increased with depth. While *Thiobacillus* is often considered aerobic, both genera of *Thiobacillus* found in this study can persist under anoxic conditions through the oxidation of ΣH_2S coupled to nitrate reduction (Townshend & White, 1960; A. Wang et al., 2005). The limited formation of Fe-sulfide minerals in P8 may reflect reduced Fe availability or rapid microbial oxidation of ΣH_2S before mineral precipitation, allowing *Thiobacillus* to thrive on freely available ΣH_2S. Thus in P8, *Thiobacillus*-mediated oxidation of ΣH_2S to SO_4^{2-} likely represents a mechanism via which continuous sulfur cycling is supported within these anoxic wetland sediments.

Variations in sulfide dynamics across sites suggest that competition between sulfate reducers and methanogens is shaped by site-specific geochemical gradients. Taxa affiliated with *Desulfobacteria* were the most abundant putative SRB within this system and likely play an important role in sulfidogenesis. Abundant ester-bound sulfate in these sediments (Tables S1 and S2 in Supporting Information S1) are not readily bioavailable, and thus the presence of sulfatase-encoding genes in *Desulfobacteria* genomes may allow these taxa to access bound sulfur through enzymatic cleavage and use the released sulfate as a terminal electron acceptor. Sulfatase enzymes were also encoded by other diverse community members that could further contribute to sulfate availability within the ecosystem. Members of the *Desulfobacteria* (i.e., Genus SpSt-501) also encoded both [NiFe] and [FeFe] hydrogenases, indicating that they likely act as H_2 scavengers in these sediments, limiting the availability of H_2 for hydrogenotrophic methanogenesis (Lovley et al., 1982). Similarly, SRB have a higher free energy yield than

Version of record at: https://doi.org/10.1029/ 2024JG008478

methanogens when using acetate as a substrate, resulting in a higher affinity for acetate and a lower abundance of acetoclastic methanogens (Lovley et al., 1982; Lovley & Klug, 1986; Muyzer & Stams, 2008).

However, the likely activity of SRB and associated production of high levels of ΣH_2S has significant impacts on other microbial metabolisms within PPR wetland sediments. High sulfide concentrations are known to cause toxicity across diverse microorganisms including SRB, thus disrupting certain functions within microbial communities (Kushkevych et al., 2019; Shakeri Yekta et al., 2023). Indeed, ΣH_2S concentrations negatively correlated with *Desulfobacteria* relative abundances (Figure 4), suggesting that these taxa are enriched in locations where ΣH_2S concentrations are lower and issues associated with sulfide toxicity may be reduced. Beyond SRB, high sulfide levels have been associated with reduced presence and activity of acetoclastic methanogens in wetlands (He et al., 2015). Thus, in addition to SRB-driven competition for substrates needed for hydrogenotrophic and acetoclastic methanogenesis in wetland P8, sulfide toxicity likely also plays a role in shaping the methanogen community and their associated activity. The location with the lowest aqueous ΣH_2S concentrations (P7A) had a higher absolute abundance of *mcrA* genes. When paired with 16S rRNA gene relative abundance data, these genes corresponded to methanogens encoding hydrogenotrophic (*Methanobacterium A*) and acetoclastic (*Methanosarcina*) pathways. In contrast, wetland P8 sediments contained the highest pore water sulfide concentrations and the lowest abundance of methanogens (inferred from *mcrA* gene abundances and 16S rRNA relative abundance data). However, these methanogen populations were dominated by methylotrophic methanogens. The depletion of hydrogenotrophic and acetoclastic methanogens in the presence of elevated sulfide mirrors studies in marine systems where H_2 and acetate act as competitive substrates for active SRB that outcompete the hydrogenotrophic and acetoclastic methanogens (Lovley et al., 1982; Muyzer & Stams, 2008). Conversely, the relative enrichment of methylotrophic methanogens in high sulfide zones may result from (a) their ability to use some methylated compounds that are considered noncompetitive substrates, allowing methylotrophic methanogenesis to co-occur with sulfate reduction (Maltby et al., 2018; Schorn et al., 2022), and (b) higher free energy yields from this methanogenic pathway, enabling the use of stress tolerance mechanisms in the face of sulfide toxicity. Some studies have reported widespread tolerance and adaptive strategies to sulfide toxicity in anaerobic microbes, such as encoding cytochrome *bd* instead of the more susceptible cytochrome c (Xia et al., 2018). However, research on the susceptibility of methanogens to sulfide toxicity across different pathways remains limited, and future studies are needed to better understand the role that sulfide toxicity may play in methanogenesis within PPR wetlands.

While competition for substrates represents one key mediator of methanogenesis, the production of these compounds also acts as a control point for methanogens. Methanogenesis is frequently supported by the activity of fermentative microorganisms which generate methanogenic substrates (e.g., acetate, H_2) as metabolic byproducts (Park et al., 2006). In wetland P7, despite lower relative abundance of putative fermenters such as *SM-150* compared to P8, we propose that cross-feeding between putative fermenters and dominant acetoclastic and hydrogenotrophic methanogens results in co-occurrence patterns across the sediment depth profile. In contrast, putative fermenter *SM-150* and dominant methylotrophic methanogens in wetland P8 displayed inverse trends in relative abundance across the depth profile (Figure S2 in Supporting Information S1), with hydrogenotrophic and acetoclastic methanogens making up a very small fraction of the methanogen community. In this instance, we propose that most fermentation byproducts support other reactions such as sulfate reduction and acetogenesis, with methylotrophic substrates sourced from other processes. Many methylotrophic substrates such as quaternary amines (e.g., glycine betaine) are found in high abundance in soils and grasslands (Warren, 2013), while methylotrophic substrates precursors such as dimethylsulfoniopropionate (precursor for DMS) (Tebbe et al., 2023) are produced by plants during abiotic stress to serve as osmoprotectants and cryoprotectants (Daly et al., 2016; Karabudak et al., 2014; Kurepin et al., 2015). Furthermore, studies have shown that DMS can be used by methanogens in the presence of sulfate and active SRB when found in high enough concentrations (S. L. Tsola et al., 2024, 2021). The wetlands in this study are surrounded by undisturbed prairie grasslands, which could be contributing methylated compounds into wetland sediments via runoff.

To fully understand CH_4 flux in a system, CH_4 oxidation in addition to production needs to be considered. In freshwater wetlands, it is estimated that methanotrophs oxidize 20%–80% of CH_4 before it is emitted, with up to 50% coming from anaerobic oxidation of CH_4 (AOM) (Jensen et al., 2023; Le Mer & Roger, 2001; Singleton et al., 2018; Zhao & Lu, 2023). This value contrasts with marine environments, where greater than 90% of biogenic CH_4 is estimated to be consumed by AOM (Hinrichs & Boetius, 2003; Knittel & Boetius, 2009; Reeburgh, 2007). In marine environments, AOM occurs through anaerobic methanotrophic archaea (ANME) coupled to sulfate reduction (S-AOM) occurring in the sulfate CH_4 transition zone. Because freshwater wetlands typically have lower sulfate concentrations (0.1–0.2 mM) than marine systems (up to 28 mM), S-AOM is generally thought to play a much smaller role in mitigating CH_4 emissions to the atmosphere. Despite high levels of sulfate in the PPR research sites, no ANME were detected in any of the samples collected suggesting S-AOM is not occurring. While ANME could exist deeper in the sediment depth profile, ANME are also susceptible to sulfide toxicity (Dalcin Martins et al., 2024; Schmitz et al., 2023). One study found that euxinic conditions (i.e., those characterized by anoxia and high conditions of sulfide) resulted in toxicity in ANME even though substrates were available within the site (Dalcin Martins et al., 2024). At the sites studied here, the varying extent of euxinia directly corresponds with historical CH_4 flux, with wetland P8 characterized by the highest sulfide concentrations and CH_4 fluxes. While neither wetlands P7 nor P8 contained evidence of ANME, aerobic methanotrophs were present in both. P7 had higher relative abundance of methanotrophs which also spanned a greater depth gradient than those observed in P8. While some methanotrophs do possess sulfide detoxification mechanisms, they may still be inhibited by the high concentrations of H_2S characteristic of P8 (Schmitz et al., 2023). Thus, we hypothesize that the low relative abundance of methanotrophs in P8 is likely attributed to sulfide toxicity, resulting in lower rates of methane oxidation in P8 compared to P7. This likely plays an important role in the higher CH_4 fluxes historically observed in P8, despite the lower diversity and abundance of methanogens. However, further exploration is needed to fully understand this relationship.

Wetlands P7 and P8 at the Cottonwood Lakes Study Area are historically two of the highest CH_4 emitting wetlands measured across the United States, although historical data reveals six times greater annual CH_4 flux from P8 relative to P7, which was measured continuously over 19 years (Tangen & Bansal, 2019). Here we propose that the regional hydrogeology and connectivity plays a key role in mediating microbial community composition and activity within these wetland sediments, with implications for carbon mineralization and CH_4 cycling. Existing within a previously glaciated area, PPR wetlands can be categorized as (a) recharge wetlands which fill through precipitation events thus helping recharge the ground water, and contain low levels of mineral derived solutes, (b) flow-through wetlands which receive water from shallow groundwater flow from recharge wetlands, and (c) discharge wetlands which receive water from groundwater discharge. Flow-through and discharge wetlands therefore have higher solute concentrations due to dissolved minerals transported by groundwater, with discharge wetlands containing the highest solute concentrations (Euliss et al., 2014; Kirby et al., 2002). In P8—a discharge wetland—historically higher sulfate concentrations (Dalcin Martins et al., 2017; Euliss et al., 2014) via both the concentration of solutes and microbial oxidation of reduced sulfur species likely support the activity of SRB. In turn, this may result in greater competition for H_2 and acetate and reduced abundance of hydrogenotrophic and acetoclastic methanogens. Within these sediments, the use of alternative substrates by methylotrophic methanogens could allow methanogenesis to continue alongside sulfate reduction. Furthermore, given that sulfide toxicity of acetoclastic methanogens has been shown in other wetland systems (He et al., 2015), the reduction of acetoclastic and hydrogenotrophic methanogens in P8 could be a result of substrate competition or sulfide toxicity and thus warrants further investigation. Finally, these higher rates of sulfate reduction and associated accumulation of sulfide in P8 may also lead to some degree of toxicity for methanotrophs, resulting in reduced rates of CH_4 oxidation. Together, these coupled microbial and geochemical processes suggest that despite high inferred rates of methanogenesis in both wetlands, the differing role of methanotrophs in the two locations (abundant in P7, absent in P8) likely results in the significant differences in CH_4 flux to the atmosphere (Figure 6; Figure S5 in Supporting Information S1).

5. Conclusions

The PPR complex, spanning millions of depressional wetlands across North America, is the tenth largest wetland complex in the world and a biogeochemical hotspot (Keddy et al., 2009). Here we studied fine-scale patterns in sediment microbiology and geochemistry to understand the factors mediating differences in CH_4 flux between adjacent wetlands. Wetland P8 was characterized by extremely high levels of sulfide, high CH_4 fluxes, and higher relative abundances of SRBs and sulfide oxidizers, but lower relative abundances of methanogens and methanotrophs. In contrast, while lower ΣH_2S concentrations in wetland P7 allowed for the persistence of acetoclastic and hydrogenotrophic methanogens, the inferred activity of methanotrophs likely acted as a key sink in controlling CH_4 emissions to the atmosphere. Overall, we attribute the highest CH_4 emissions across these wetlands to methylotrophic methanogenesis, an underappreciated methanogenesis pathway, co-occurring alongside high levels of sulfate reduction resulting in an environment where high levels of methane production occurs in the near

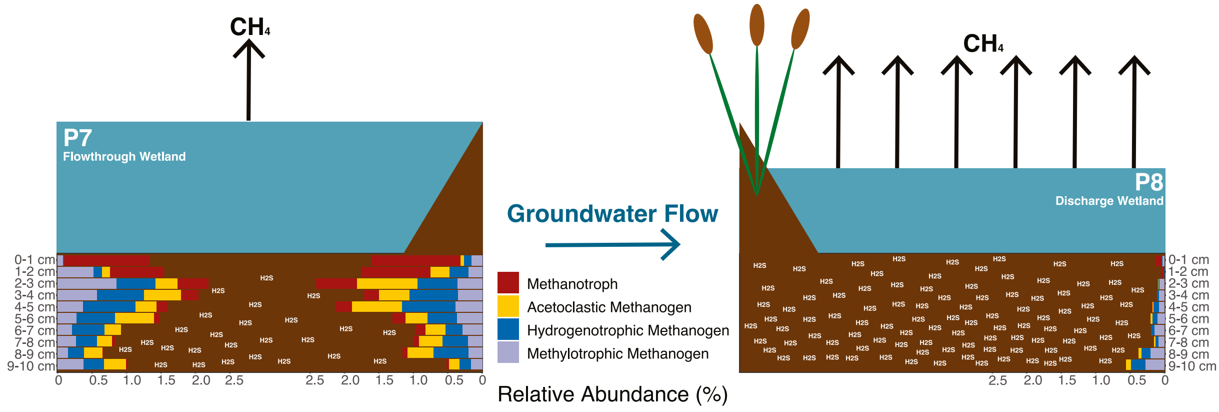

Figure 6. A conceptual figure of the microbial community and pore water chemistry measured in wetlands P7 (two locations) and P8. H_2S is scaled based on measurements taken in this study presented in Figure 1 and CH_4 annotations are scaled based on historical environmental measurements. Previous work reported annual CH_4 flux in P8 was 603.25 g C m^{-2} yr^{-1} compared to 101.48 g C m^{-2} yr^{-1} in P7 (Tangen & Bansal, 2019). Relative abundances of methanogens are provided for each pathway (acetoclasts are illustrated in yellow, hydrogenotrophs in blue, and methylotrophs in purple) and relative abundances of methanotrophs are provided in red.

absence of sediment methane oxidation. Moving forward, understanding how sulfide toxicity and methanogenesis pathways contribute to CH_4 flux in these environments will enable a better understanding of regional and global CH_4 budgets.

Data Availability Statement

The bacterial and archaeal 16S rRNA gene sequencing reads utilized in this manuscript have been deposited in the National Center for Biotechnology Information (NBCI) PRJNA1007388. Additionally, all MAGs (only MAGs from PPR were included) and their DRAM v1.3.2 annotations and the newick trees for phylogenomic and phylogenetic analyses, and a curated list of methanogens and methanotrophs used in this paper were from a previous publication and are available on Zenodo (https://zenodo.org/records/14532347) (E. Bechtold et al., 2024). Flux data is given in a previous publication (Tangen & Bansal, 2019).

Acknowledgments

Funding for this work was provided by the National Science Foundation (Projects 2029645 (MP, BMT, WAA), 2029665 (DX, YPC), 2029686 (EKB, MJW)) and by U.S. Department of Energy (DOE) Office of Science, Office of Biological and Environmental Research (BER) grant DE-SC0023084 (EKB, MJW). A portion of the research described in this paper was performed using Beamline 06B1-1 (SXRMB) at the Canadian Light Source, a national research facility of the University of Saskatchewan, which is supported by the Canada Foundation for Innovation (CFI), the Natural Sciences and Engineering Research Council (NSERC), the National Research Council (NRC), the Canadian Institutes of Health Research (CIHR), the Government of Saskatchewan, and the University of Saskatchewan. Thanks to beamline scientist Mohsen Shakouri for assisting in synchrotron data collection. A portion of this research used Beamline 7-BM (QAS) of the National Synchrotron Light Source II, a U.S. Department of Energy (DOE) Office of Science User Facility operated for the DOE Office of Science by Brookhaven National Laboratory under Contract No. DE-SC0012704. Thanks to beamline scientists Lu Ma and Stephen Ehrlich for their support. The authors thank Matthew Solensky and Sheel Bansal from the USGS, Anthony Sigman-Lowery (University of Delaware) and Cole Stenberg (UMN) for assistance with field sampling and helpful discussions.

References

Angle, J. C., Morin, T. H., Solden, L. M., Narrowe, A. B., Smith, G. J., Borton, M. A., et al. (2017). Methanogenesis in oxygenated soils is a substantial fraction of wetland methane emissions. *Nature Communications*, *8*(1), 1567. https://doi.org/10.1038/s41467-017-01753-4

Apprill, A., McNally, S., Parsons, R., & Weber, L. (2015). Minor revision to V4 region SSU rRNA 806R gene primer greatly increases detection of SAR11 bacterioplankton. *Aquatic Microbial Ecology*, *75*(2), 129–137. https://doi.org/10.3354/ame01753

Arnold, W., Taylor, M., Bradford, M., Raymond, P., & Peccia, J. (2023). Microbial activity contributes to spatial heterogeneity of wetland methane fluxes. *Microbiology Spectrum*, *11*(5), e0271423. https://doi.org/10.1128/spectrum.02714-23

Bansal, S., Post van der Burg, M., Fern, R. R., Jones, J. W., Lo, R., McKenna, O. P., et al. (2023). Large increases in methane emissions expected from North America's largest wetland complex. *Science Advances*, *9*(9), eade1112. https://doi.org/10.1126/sciadv.ade1112

Bansal, S., Tangen, B., & Finocchiaro, R. (2016). Temperature and hydrology affect methane emissions from prairie pothole wetlands. *Wetlands*, *36*(S2), 371–381. https://doi.org/10.1007/s13157-016-0826-8

Barbeyron, T., Potin, P., Richard, C., Collin, O., & Kloareg, B. (1995). Arylsulphatase from Alteromonas carrageenovora. *Microbiology*, *141*(11), 2897–2904. https://doi.org/10.1099/13500872-141-11-2897

Bartlett, K. B., Bartlett, D. S., Harriss, R. C., & Sebacher, D. I. (1987). Methane emissions along a salt marsh salinity gradient. *Biogeochemistry*, *4*(3), 183–202. https://doi.org/10.1007/BF02187365

Bechtold, E., Wrighton, K., & Wilkins, M. (2024). Multi-omics for understanding climate change (MUCC) database v2.0.0 [Dataset]. *Zenodo*. https://doi.org/10.5281/zenodo.10822869

Bechtold, E. K., Ellenbogen, J. B., Villa, J. A., de Melo Ferreira, D. K., Oliverio, A. M., Kostka, J. E., et al. (2025). Metabolic interactions underpinning high methane fluxes across terrestrial freshwater wetlands. *Nature Communications*, *16*(1), 944. https://doi.org/10.1038/s41467-025-56133-0

Beeri, O., & Phillips, R. L. (2007). Tracking palustrine water seasonal and annual variability in agricultural wetland landscapes using Landsat from 1997 to 2005. *Global Change Biology*, *13*(4), 897–912. https://doi.org/10.1111/j.1365-2486.2006.01306.x

Benjamini, Y., & Hochberg, Y. (1995). Controlling the false discovery rate: A practical and powerful approach to multiple testing. *Journal of the Royal Statistical Society: Series B*, *57*(1), 289–300. https://doi.org/10.1111/j.2517-6161.1995.tb02031.x

Bridgham, S. D., Cadillo-Quiroz, H., Keller, J. K., & Zhuang, Q. (2013). Methane emissions from wetlands: Biogeochemical, microbial, and modeling perspectives from local to global scales. *Global Change Biology*, *19*(5), 1325–1346. https://doi.org/10.1111/gcb.12131

Burgin, A. J., Yang, W. H., Hamilton, S. K., & Silver, W. L. (2011). Beyond carbon and nitrogen: How the microbial energy economy couples elemental cycles in diverse ecosystems. *Frontiers in Ecology and the Environment*, *9*(1), 44–52. https://doi.org/10.1890/090227

Capone, D. G., & Kiene, R. P. (1988). Comparison of microbial dynamics in marine and freshwater sediments: Contrasts in anaerobic carbon catabolism1. *Limnology & Oceanography*, *33*(4part2), 725–749. https://doi.org/10.4319/lo.1988.33.4part2.0725

Chaumeil, P.-A., Mussig, A. J., Hugenholtz, P., & Parks, D. H. (2020). GTDB-Tk: A toolkit to classify genomes with the Genome Taxonomy Database. *Bioinformatics*, *36*(6), 1925–1927. https://doi.org/10.1093/bioinformatics/btz848

Chen, J., Hanke, A., Tegetmeyer, H. E., Kattelmann, I., Sharma, R., Hamann, E., et al. (2017). Impacts of chemical gradients on microbial community structure. *The ISME Journal*, *11*(4), 920–931. https://doi.org/10.1038/ismej.2016.175

Chin, Y.-P., McKnight, D. M., D'Andrilli, J., Brooks, N., Cawley, K., Guerard, J., et al. (2023). Identification of next-generation International Humic Substances Society reference materials for advancing the understanding of the role of natural organic matter in the Anthropocene. *Aquatic Sciences*, *85*(1), 32. https://doi.org/10.1007/s00027-022-00923-x

Cozannet, M., Le Guellec, S., & Alain, K. (2023). A variety of substrates for methanogenesis. *Case Studies in Chemical and Environmental Engineering*, *8*, 100533. https://doi.org/10.1016/j.cscee.2023.100533

Cron, B. R., Sheik, C. S., Kafantaris, F.-C. A., Druschel, G. K., Seewald, J. S., German, C. R., et al. (2020). Dynamic biogeochemistry of the particulate sulfur pool in a buoyant deep-sea hydrothermal plume. *ACS Earth and Space Chemistry*, *4*(2), 168–182. https://doi.org/10.1021/acsearthspacechem.9b00214

Dalcin Martins, P., de Monlevad, J. P. R. C., Echeveste Medrano, M. J., Lenstra, W. K., Wallenius, A. J., Hermans, M., et al. (2024). Sulfide toxicity as key control on anaerobic oxidation of methane in eutrophic coastal sediments. *Environmental Science & Technology*, *58*(26), 11421–11435. https://doi.org/10.1021/acs.est.3c10418

Dalcin Martins, P., Hoyt, D. W., Bansal, S., Mills, C. T., Tfaily, M., Tangen, B. A., et al. (2017). Abundant carbon substrates drive extremely high sulfate reduction rates and methane fluxes in Prairie Pothole Wetlands. *Global Change Biology*, *23*(8), 3107–3120. https://doi.org/10.1111/gcb.13633

Daly, R. A., Borton, M. A., Wilkins, M. J., Hoyt, D. W., Kountz, D. J., Wolfe, R. A., et al. (2016). Microbial metabolisms in a 2.5-km-deep ecosystem created by hydraulic fracturing in shales. *Nature Microbiology*, *1*(10), 1–9. https://doi.org/10.1038/nmicrobiol.2016.146

Delwiche, K. B., Knox, S. H., Malhotra, A., Fluet-Chouinard, E., McNicol, G., Feron, S., et al. (2021). FLUXNET-CH_4: A global, multi-ecosystem dataset and analysis of methane seasonality from freshwater wetlands. *Earth System Science Data*, *13*(7), 3607–3689. https://doi.org/10.5194/essd-13-3607-2021

Ellenbogen, J. B., Borton, M. A., McGivern, B. B., Cronin, D. R., Hoyt, D. W., Freire-Zapata, V., et al. (2023). Methylotrophy in the Mire: Direct and indirect routes for methane production in thawing permafrost. *mSystems*, *9*(1), e00698-23. https://doi.org/10.1128/msystems.00698-23

Euliss, N. H., Mushet, D. M., Newton, W. E., Otto, C. R. V., Nelson, R. D., LaBaugh, J. W., et al. (2014). Placing prairie pothole wetlands along spatial and temporal continua to improve integration of wetland function in ecological investigations. *Journal of Hydrology*, *513*, 490–503. https://doi.org/10.1016/j.jhydrol.2014.04.006

Goldhaber, M. B., Mills, C. T., Morrison, J. M., Stricker, C. A., Mushet, D. M., & LaBaugh, J. W. (2014). Hydrogeochemistry of prairie pothole region wetlands: Role of long-term critical zone processes. *Chemical Geology*, *387*, 170–183. https://doi.org/10.1016/j.chemgeo.2014.08.023

Gramp, J. P., Bigham, J. M., Jones, F. S., & Tuovinen, O. H. (2010). Formation of Fe-sulfides in cultures of sulfate-reducing bacteria. *Journal of Hazardous Materials*, *175*(1), 1062–1067. https://doi.org/10.1016/j.jhazmat.2009.10.119

Grant, R. F. (1998). Simulation of methanogenesis in the mathematical model *ecosys*. *Soil Biology and Biochemistry*, *30*(7), 883–896. https://doi.org/10.1016/S0038-0717(97)00218-6

Grant, R. F., Mekonnen, Z. A., Riley, W. J., Arora, B., & Torn, M. S. (2017). Mathematical modelling of Arctic Polygonal tundra with ecosys: 2. Microtopography determines how CO2 and CH4 exchange responds to changes in temperature and precipitation. *Journal of Geophysical Research: Biogeosciences*, *122*(12), 3174–3187. https://doi.org/10.1002/2017JG004037

Hakala, J. A., Fimmen, R. L., Chin, Y.-P., Agrawal, S. G., & Ward, C. P. (2009). Assessment of the geochemical reactivity of Fe-DOM complexes in wetland sediment pore waters using a nitroaromatic probe compound. *Geochimica et Cosmochimica Acta*, *73*(5), 1382–1393. https://doi.org/10.1016/j.gca.2008.12.001

Hartman, W. H., Bueno de Mesquita, C. P., Theroux, S. M., Morgan-Lang, C., Baldocchi, D. D., & Tringe, S. G. (2024). Multiple microbial guilds mediate soil methane cycling along a wetland salinity gradient. *mSystems*, *9*(1), e00936-23. https://doi.org/10.1128/msystems.00936-23

He, S., Malfatti, S. A., McFarland, J. W., Anderson, F. E., Pati, A., Huntemann, M., et al. (2015). Patterns in wetland microbial community composition and functional gene repertoire associated with methane emissions. *mBio*, *6*(3), e00066-00015. https://doi.org/10.1128/mBio.00066-15

Hinrichs, K.-U., & Boetius, A. (2003). The anaerobic oxidation of methane: New insights in microbial ecology and biogeochemistry. In G. Wefer, D. Billett, D. Hebbeln, B. B. Jørgensen, M. Schlüter, & T. C. E. van Weering (Eds.), *Ocean margin systems* (pp. 457–477). Springer. https://doi.org/10.1007/978-3-662-05127-6_28

Holgerson, M. A., & Raymond, P. A. (2016). Large contribution to inland water CO2 and CH4 emissions from very small ponds. *Nature Geoscience*, *9*(3), 222–226. https://doi.org/10.1038/ngeo2654

Hudson, J. M., Michaud, A. B., Emerson, D., & Chin, Y.-P. (2022). Spatial distribution and biogeochemistry of redox active species in arctic sedimentary porewaters and seeps. *Environmental Sciences: Processes & Impacts*, *24*(3), 426–438. https://doi.org/10.1039/D1EM00505G

Jensen, S., Siljanen, H. M. P., & Dörsch, P. (2023). Activity and abundance of methanotrophic bacteria in a northern mountainous gradient of wetlands. *Environmental Microbiology Reports*, *15*(3), 206–215. https://doi.org/10.1111/1758-2229.13137

Jørgensen, B., & Kasten, S. (2006). Sulfur cycling and methane oxidation. In *Marine geochemistry* (pp. 271–309). https://doi.org/10.1007/3-540-32144-6_8

Karabudak, T., Bor, M., Özdemir, F., & Türkan, İ. (2014). Glycine betaine protects tomato (Solanum lycopersicum) plants at low temperature by inducing fatty acid desaturase7 and lipoxygenase gene expression. *Molecular Biology Reports*, *41*(3), 1401–1410. https://doi.org/10.1007/s11033-013-2984-6

Kassambara, A. (2023). ggpubr: "ggplot2" based publication ready plots (Version 0.6.0). Retrieved from https://cran.r-project.org/web/packages/ggpubr/index.html

Keddy, P. A., Fraser, L. H., Solomeshch, A. I., Junk, W. J., Campbell, D. R., Arroyo, M. T. K., & Alho, C. J. R. (2009). Wet and wonderful: The world's largest wetlands are conservation priorities. *BioScience*, *59*(1), 39–51. https://doi.org/10.1525/bio.2009.59.1.8

King, G. M. (1984). Metabolism of trimethylamine, choline, and glycine betaine by sulfate-reducing and methanogenic bacteria in marine sediments. *Applied and Environmental Microbiology*, *48*(4), 719–725. https://doi.org/10.1128/aem.48.4.719-725.1984

Kirby, D. R., Krabbenhoft, K. D., & Sedivec, K. K., & Society for Range Management. (2002). Wetlands in northern plains prairies: Offer societal values too. *Rangelands*, *24*(2). https://doi.org/10.2458/azu_rangelands_v24i2_kirby2

Knittel, K., & Boetius, A. (2009). Anaerobic oxidation of methane: Progress with an unknown process. *Annual Review of Microbiology*, *63*(1), 311–334. https://doi.org/10.1146/annurev.micro.61.080706.093130

Kurepin, L. V., Ivanov, A. G., Zaman, M., Pharis, R. P., Allakhverdiev, S. I., Hurry, V., & Hüner, N. P. A. (2015). Stress-related hormones and glycinebetaine interplay in protection of photosynthesis under abiotic stress conditions. *Photosynthesis Research*, *126*(2), 221–235. https://doi.org/10.1007/s11120-015-0125-x

Journal of Geophysical Research: Biogeosciences 10.1029/2024JG008478

Kurth, J. M., Nobu, M. K., Tamaki, H., de Jonge, N., Berger, S., Jetten, M. S. M., et al. (2021). Methanogenic archaea use a bacteria-like methyltransferase system to demethoxylate aromatic compounds. *The ISME Journal*, *15*(12), 3549–3565. https://doi.org/10.1038/s41396-021-01025-6

Kurth, J. M., Op den Camp, H. J. M., & Welte, C. U. (2020). Several ways one goal—methanogenesis from unconventional substrates. *Applied Microbiology and Biotechnology*, *104*(16), 6839–6854. https://doi.org/10.1007/s00253-020-10724-7

Kushkevych, I., Dordević, D., & Vítězová, M. (2019). Toxicity of hydrogen sulfide toward sulfate-reducing bacteria Desulfovibrio piger Vib-7. *Archives of Microbiology*, *201*(3), 389–397. https://doi.org/10.1007/s00203-019-01625-z

Laanbroek, H. J. (2010). Methane emission from natural wetlands: Interplay between emergent macrophytes and soil microbial processes. A mini-review. *Annals of Botany*, *105*(1), 141–153. https://doi.org/10.1093/aob/mcp201

Le Mer, J., & Roger, P. (2001). Production, oxidation, emission and consumption of methane by soils: A review. *European Journal of Soil Biology*, *37*(1), 25–50. https://doi.org/10.1016/S1164-5563(01)01067-6

Liu, Y., & Whitman, W. B. (2008). Metabolic, phylogenetic, and ecological diversity of the methanogenic archaea. *Annals of the New York Academy of Sciences*, *1125*(1), 171–189. https://doi.org/10.1196/annals.1419.019

Lovley, D. R., Dwyer, D. F., & Klug, M. J. (1982). Kinetic analysis of competition between sulfate reducers and methanogens for hydrogen in sediments. *Applied and Environmental Microbiology*, *43*(6), 1373–1379. https://doi.org/10.1128/aem.43.6.1373-1379.1982

Lovley, D. R., & Klug, M. J. (1986). Model for the distribution of sulfate reduction and methanogenesis in freshwater sediments. *Geochimica et Cosmochimica Acta*, *50*(1), 11–18. https://doi.org/10.1016/0016-7037(86)90043-8

Luther, G. W., Glazer, B. T., Ma, S., Trouwborst, R. E., Moore, T. S., Metzger, E., et al. (2008). Use of voltammetric solid-state (micro)electrodes for studying biogeochemical processes: Laboratory measurements to real time measurements with an *in situ* electrochemical analyzer (ISEA). *Marine Chemistry*, *108*(3), 221–235. https://doi.org/10.1016/j.marchem.2007.03.002

Ma, S., Luther III, G. W., Keller, J., Madison, A. S., Metzger, E., Emerson, D., & Megonigal, J. P. (2008). Solid-state Au/Hg microelectrode for the investigation of Fe and Mn cycling in a freshwater wetland: Implications for methane production. *Electroanalysis*, *20*(3), 233–239. https://doi.org/10.1002/elan.200704048

Maltby, J., Steinle, L., Löscher, C. R., Bange, H. W., Fischer, M. A., Schmidt, M., & Treude, T. (2018). Microbial methanogenesis in the sulfate-reducing zone of sediments in the Eckernförde Bay, SW Baltic Sea. *Biogeosciences*, *15*(1), 137–157. https://doi.org/10.5194/bg-15-137-2018

Manceau, A., Marcus, M. A., & Tamura, N. (2002). Quantitative speciation of heavy metals in soils and sediments by synchrotron X-ray techniques. *Reviews in Mineralogy and Geochemistry*, *49*(1), 341–428. https://doi.org/10.2138/gsrmg.49.1.341

Marcus, M. A., MacDowell, A. A., Celestre, R., Manceau, A., Miller, T., Padmore, H. A., & Sublett, R. E. (2004). Beamline 10.3.2 at ALS: A hard X-ray microprobe for environmental and materials sciences. *Journal of Synchrotron Radiation*, *11*(Pt 3), 239–247. https://doi.org/10.1107/S0909049504005837

Marcus, M. A., Westphal, A. J., & Fakra, S. C. (2008). Classification of Fe-bearing species from K-edge XANES data using two-parameter correlation plots. *Journal of Synchrotron Radiation*, *15*(Pt 5), 463–468. https://doi.org/10.1107/S0909049508018293

McAdams, B. C., Adams, R. M., Arnold, W. A., & Chin, Y.-P. (2016). Novel insights into the distribution of reduced sulfur species in prairie pothole wetland pore waters provided by bismuth film electrodes. *Environmental Science and Technology Letters*, *3*(3), 104–109. https://doi.org/10.1021/acs.estlett.6b00020

Mobilian, C., & Craft, C. B. (2022). Wetland soils: Physical and chemical properties and biogeochemical processes. In T. Mehner & K. Tockner (Eds.), *Encyclopedia of inland waters* (2nd ed., pp. 157–168). Elsevier. https://doi.org/10.1016/B978-0-12-819166-8.00049-9

Mondav, R., Woodcroft, B. J., Kim, E.-H., McCalley, C. K., Hodgkins, S. B., Crill, P. M., et al. (2014). Discovery of a novel methanogen prevalent in thawing permafrost. *Nature Communications*, *5*(1), 3212. https://doi.org/10.1038/ncomms4212

Muyzer, G., & Stams, A. J. M. (2008). The ecology and biotechnology of sulphate-reducing bacteria. *Nature Reviews Microbiology*, *6*(6), 441–454. https://doi.org/10.1038/nrmicro1892

Narihiro, T., & Sekiguchi, Y. (2011). Oligonucleotide primers, probes and molecular methods for the environmental monitoring of methanogenic archaea. *Microbial Biotechnology*, *4*(5), 585–602. https://doi.org/10.1111/j.1751-7915.2010.00239.x

Narrowe, A. B., Borton, M. A., Hoyt, D. W., Smith, G. J., Daly, R. A., Angle, J. C., et al. (2019). Uncovering the diversity and activity of methylotrophic methanogens in freshwater wetland soils. *mSystems*, *4*(6), e00320-19. https://doi.org/10.1128/mSystems.00320-19

Oksanen, J., Blanchet, F. G., Friendly, M., Kindt, R., Legendre, P., McGlinn, D., et al. (2019). Vegan: Community ecology package (version 2.5-6). Retrieved from https://CRAN.R-project.org/package=vegan

Oliverio, A. M., Narrowe, A. B., Villa, J. A., Rinke, C., Hoyt, D. W., Liu, P., et al. (2024). Rendering the metabolic wiring powering wetland soil methane production. *bioRxiv*. https://doi.org/10.1101/2024.02.06.579222

Oremland, R. S., Marsh, L. M., & Polcin, S. (1982). Methane production and simultaneous sulphate reduction in anoxic, salt marsh sediments. *Nature*, *296*(5853), 143–145. https://doi.org/10.1038/296143a0

Parada, A. E., Needham, D. M., & Fuhrman, J. A. (2016). Every base matters: Assessing small subunit rRNA primers for marine microbiomes with mock communities, time series and global field samples. *Environmental Microbiology*, *18*(5), 1403–1414. https://doi.org/10.1111/1462-2920.13023

Park, J., Sanford, R. A., & Bethke, C. M. (2006). Geochemical and microbiological zonation of the Middendorf aquifer, South Carolina. *Chemical Geology*, *230*(1), 88–104. https://doi.org/10.1016/j.chemgeo.2005.12.001

Peiffer, S., Kappler, A., Haderlein, S. B., Schmidt, C., Byrne, J. M., Kleindienst, S., et al. (2021). A biogeochemical–hydrological framework for the role of redox-active compounds in aquatic systems. *Nature Geoscience*, *14*(5), 264–272. https://doi.org/10.1038/s41561-021-00742-z

Pennock, D., Yates, T., Bedard-Haughn, A., Phipps, K., Farrell, R., & McDougal, R. (2010). Landscape controls on N2O and CH4 emissions from freshwater mineral soil wetlands of the Canadian Prairie Pothole region. *Geoderma*, *155*(3), 308–319. https://doi.org/10.1016/j.geoderma.2009.12.015

Pierce, C. E., Furman, O. S., Nicholas, S. L., Wasik, J. C., Gionfriddo, C. M., Wymore, A. M., et al. (2022). Role of ester sulfate and organic disulfide in Mercury methylation in Peatland soils. *Environmental Science & Technology*, *56*(2), 1433–1444. https://doi.org/10.1021/acs.est.1c04662

Quast, C., Pruesse, E., Yilmaz, P., Gerken, J., Schweer, T., Yarza, P., et al. (2013). The SILVA ribosomal RNA gene database project: Improved data processing and web-based tools. *Nucleic Acids Research*, *41*(Database issue), D590–D596. https://doi.org/10.1093/nar/gks1219

Ravel, B., & Newville, M. (2005). ATHENA and ARTEMIS: Interactive graphical data analysis using IFEFFIT. *Physica Scripta*, *2005*(T115), 1007. https://doi.org/10.1238/Physica.Topical.115a01007

Reeburgh, W. S. (2007). Oceanic methane biogeochemistry. *Chemical Reviews*, *107*(2), 486–513. https://doi.org/10.1021/cr050362v

Rosentreter, J. A., Borges, A. V., Deemer, B. R., Holgerson, M. A., Liu, S., Song, C., et al. (2021). Half of global methane emissions come from highly variable aquatic ecosystem sources. *Nature Geoscience*, *14*(4), 225–230. https://doi.org/10.1038/s41561-021-00715-2

Schmitz, R. A., Peeters, S. H., Mohammadi, S. S., Berben, T., van Erven, T., Iosif, C. A., et al. (2023). Simultaneous sulfide and methane oxidation by an extremophile. *Nature Communications*, *14*(1), 2974. https://doi.org/10.1038/s41467-023-38699-9

Schorn, S., Ahmerkamp, S., Bullock, E., Weber, M., Lott, C., Liebeke, M., et al. (2022). Diverse methylotrophic methanogenic archaea cause high methane emissions from seagrass meadows. *Proceedings of the National Academy of Sciences*, *119*(9), e2106628119. https://doi.org/10.1073/pnas.2106628119

Seelig, B., & DeKeyser, S. (2006). Water quality and wetland function. Retrieved from https://api.semanticscholar.org/CorpusID:130649513

Sela-Adler, M., Ronen, Z., Herut, B., Antler, G., Vigderovich, H., Eckert, W., & Sivan, O. (2017). Co-existence of methanogenesis and sulfate reduction with common substrates in sulfate-rich estuarine sediments. *Frontiers in Microbiology*, *8*, 766. https://doi.org/10.3389/fmicb.2017.00766

Shaffer, M., Borton, M. A., McGivern, B. B., Zayed, A. A., La Rosa, S. L., Solden, L. M., et al. (2020). DRAM for distilling microbial metabolism to automate the curation of microbiome function. *Nucleic Acids Research*, *48*(16), 8883–8900. https://doi.org/10.1093/nar/gkaa621

Shakeri Yekta, S., Svensson, B. H., Skyllberg, U., & Schnürer, A. (2023). Sulfide in engineered methanogenic systems – Friend or foe? *Biotechnology Advances*, *69*, 108249. https://doi.org/10.1016/j.biotechadv.2023.108249

Singleton, C. M., McCalley, C. K., Woodcroft, B. J., Boyd, J. A., Evans, P. N., Hodgkins, S. B., et al. (2018). Methanotrophy across a natural permafrost thaw environment. *The ISME Journal*, *12*(10), 2544–2558. https://doi.org/10.1038/s41396-018-0065-5

Stam, M., Lelièvre, P., Hoebeke, M., Corre, E., Barbeyron, T., & Michel, G. (2023). SulfAtlas, the sulfatase database: State of the art and new developments. *Nucleic Acids Research*, *51*(D1), D647–D653. https://doi.org/10.1093/nar/gkac977

Stewart, B. D., Sorensen, J. V., Wendt, K., Sylvan, J. B., German, C. R., Anantharaman, K., et al. (2021). A multi-modal approach to measuring particulate iron speciation in buoyant hydrothermal plumes. *Chemical Geology*, *560*, 120018. https://doi.org/10.1016/j.chemgeo.2020.120018

Tangen, B. A., & Bansal, S. (2019). Soil properties and greenhouse gas fluxes of Prairie Pothole Region wetlands: A comprehensive data release: U.S. Geological Survey data release [Dataset]. https://doi.org/10.5066/F7KS6QG2

Tebbe, D. A., Gruender, C., Dlugosch, L., Lõhmus, K., Rolfes, S., Könneke, M., et al. (2023). Microbial drivers of DMSO reduction and DMS-dependent methanogenesis in saltmarsh sediments. *The ISME Journal*, *17*(12), 2340–2351. https://doi.org/10.1038/s41396-023-01539-1

Townshend, M., & White, D. (1960). Characteristics of Thiobacillus thioparus. *Nature*, *185*(4716), 870. https://doi.org/10.1038/185870a0

Trimarco, T., Brummer, J. E., Buchanan, C., & Ippolito, J. A. (2023). Tracking soil health changes in a management-intensive grazing agro-ecosystem. *Soil Systems*, *7*(4), 94. https://doi.org/10.3390/soilsystems7040094

Tsola, S. L., Zhu, Y., Chen, Y., Sanders, I. A., Economou, C. K., Brüchert, V., & Eyice, Ö. (2024). Methanolobus use unspecific methyltransferases to produce methane from dimethylsulphide in Baltic Sea sediments. *Microbiome*, *12*(1), 3. https://doi.org/10.1186/s40168-023-01720-w

Tsola, S. L., Zhu, Y., Ghurnee, O., Economou, C. K., Trimmer, M., & Eyice, Ö. (2021). Diversity of dimethylsulfide-degrading methanogens and sulfate-reducing bacteria in anoxic sediments along the Medway Estuary, UK. *Environmental Microbiology*, *23*(8), 4434–4449. https://doi.org/10.1111/1462-2920.15637

Van Stempvoort, D. R., Hendry, M. J., Schoenau, J. J., & Krouse, H. R. (1994). Sources and dynamics of sulfur in weathered till, Western Glaciated Plains of North America. *Chemical Geology*, *111*(1), 35–56. https://doi.org/10.1016/0009-2541(94)90081-7

Waite, T. J., Kraiya, C., Trouwborst, R. E., Ma, S., & Luther III, G. W. (2006). An investigation into the suitability of bismuth as an alternative to gold-amalgam as a working electrode for the in situ determination of chemical redox species in the natural environment. *Electroanalysis*, *18*(12), 1167–1172. https://doi.org/10.1002/elan.200603519

Wang, A., Du, D., Ren, N., & van Groenestijn, J. W. (2005). An innovative process of simultaneous desulfurization and denitrification by Thiobacillus denitrificans. *Journal of Environmental Science and Health - Part A: Toxic/Hazardous Substances & Environmental Engineering*, *40*(10), 1939–1949. https://doi.org/10.1080/10934520500184590

Wang, Z., Zeng, D., & Patrick, W. H. (1996). Methane emissions from natural wetlands. *Environmental Monitoring and Assessment*, *42*(1), 143–161. https://doi.org/10.1007/BF00394047

Warren, C. R. (2013). Quaternary ammonium compounds can be abundant in some soils and are taken up as intact molecules by plants. *New Phytologist*, *198*(2), 476–485. https://doi.org/10.1111/nph.12171

Weston, N. B., Vile, M. A., Neubauer, S. C., & Velinsky, D. J. (2011). Accelerated microbial organic matter mineralization following salt-water intrusion into tidal freshwater marsh soils. *Biogeochemistry*, *102*(1), 135–151. https://doi.org/10.1007/s10533-010-9427-4

Wickham, H. (2016). *ggplot2: Elegant graphics for data analysis*. Springer-Verlag. Retrieved from https://ggplot2.tidyverse.org

Winter, T. C., & Rosenberry, D. O. (1998). Hydrology of prairie pothole wetlands during drought and deluge: A 17-Year study of the Cottonwood Lake wetland complex in North Dakota in the perspective of longer term measured and proxy hydrological records. *Climatic Change*, *40*(2), 189–209. https://doi.org/10.1023/A:1005448416571

Xia, X., Wu, S., Li, L., Xu, B., & Wang, G. (2018). The cytochrome bd complex is essential for chromate and sulfide resistance and is regulated by a GbsR-Type regulator, CydE, in Alishewanella Sp. WH16-1. *Frontiers in Microbiology*, *9*, 1849. https://doi.org/10.3389/fmicb.2018.01849

Zeng, T., Arnold, W. A., & Toner, B. M. (2013). Microscale characterization of sulfur speciation in Lake sediments. *Environmental Science & Technology*, *47*(3), 1287–1296. https://doi.org/10.1021/es303914q

Zhao, Q., & Lu, Y. (2023). Anaerobic oxidation of methane in terrestrial wetlands: The rate, identity and metabolism. *Science of the Total Environment*, *902*, 166049. https://doi.org/10.1016/j.scitotenv.2023.166049

References From the Supporting Information

Guerrero-Cruz, S., Vaksmaa, A., Horn, M. A., Niemann, H., Pijuan, M., & Ho, A. (2021). Methanotrophs: Discoveries, environmental relevance, and a perspective on current and future applications. *Frontiers in Microbiology*, *12*, 678057. https://doi.org/10.3389/fmicb.2021.678057

Liu, Y.-F., Chen, J., Liu, Z.-L., Shou, L.-B., Lin, D.-D., Zhou, L., et al. (2020). Anaerobic degradation of paraffins by thermophilic actinobacteria under methanogenic conditions. *Environmental Science & Technology*, *54*(17), 10610–10620. https://doi.org/10.1021/acs.est.0c02071

Lü, Z., & Lu, Y. (2012). Complete genome sequence of a thermophilic methanogen, Methanocella conradii HZ254, isolated from Chinese rice field soil. *Journal of Bacteriology*, *194*(9), 2398–2399. https://doi.org/10.1128/jb.00207-12